sustainability

MDPI

Article

Parameter Extraction of Solar Photovoltaic Modules Using a Novel Bio-Inspired Swarm Intelligence Optimisation Algorithm

Ram Ishwar Vais [1], Kuldeep Sahay [2], Tirumalasetty Chiranjeevi [1], Ramesh Devarapalli [3] and Łukasz Knypiński [4,*]

[1] Department of Electrical Engineering, Rajkiya Engineering College, Sonbhadra 231206, Uttar Pradesh, India
[2] Department of Electrical Engineering, Institute of Engineering and Technology, Lucknow 226021, Uttar Pradesh, India
[3] Department of Electrical/Electronics and Instrumentation Engineering, Institute of Chemical Technology, Indianoil Odisha Campus, Bhubaneswar 751013, India
[4] Faculty of Automatic Control, Robotic and Electrical Engineering, Poznan University of Technology, 60-965 Poznan, Poland
* Correspondence: lukasz.knypinski@put.poznan.pl

Abstract: For extracting the equivalent circuit parameters of solar photovoltaic (PV) panels, a unique bio-inspired swarm intelligence optimisation algorithm (OA) called the dandelion optimisation algorithm (DOA) is proposed in this study. The suggested approach has been used to analyse well-known single-diode (SD) and double-diode (DD) PV models for several PV module types, including monocrystalline SF430M, polycrystalline SG350P, and thin-film Shell ST40. The DOA is adopted by minimizing the sum of the squares of the errors at three locations (short-circuit, open-circuit, and maximum power points). Different runs are conducted to analyse the nature of the extracted parameters and the *V–I* characteristics of the PV panels under consideration. Obtained results show that for Mono SF430M, the error in the SD model is 2.5118e-19, and the error in the DD model is 2.0463e-22; for Poly SG350P, the error in the SD model is 9.4824e-21, and the error in the DD model is 2.1134e-20; for thin-film Shell ST40, the error in the SD model is 1.7621e-20, and the error in DD model is 7.9361e-22. The parameters produced from the suggested method yield the least amount of error across several executions, which suggests its better implementation in the current situation. Furthermore, statistical analysis of the SD and DD models using DOA is also carried out and compared with two hybrid OAs in the literature. Statistical results show that the standard deviation, sum, mean, and variance of various PV panels using DOA are lower compared to those of the other two hybrid OAs.

Keywords: dandelion optimisation algorithm; solar PV module; parameter estimation; single-diode model; double-diode model

Citation: Vais, R.I.; Sahay, K.; Chiranjeevi, T.; Devarapalli, R.; Knypiński, Ł. Parameter Extraction of Solar Photovoltaic Modules Using a Novel Bio-Inspired Swarm Intelligence Optimisation Algorithm. *Sustainability* **2023**, *15*, 8407. https://doi.org/10.3390/su15108407

Academic Editors: Luis Hernández-Callejo, Yao Yu and Abdulaziz Banawi

Received: 22 February 2023
Revised: 8 May 2023
Accepted: 19 May 2023
Published: 22 May 2023

1. Introduction

Various aspects of human existence are becoming progressively dominated by renewable energy as a viable replacement for fossil fuels [1–3]. Researchers have been inspired by solar energy since it is renewable, accessible, ecologically benign, and simple to install and maintain [4–6]. To be more specific, PV cells significantly contribute to the conversion of solar radiation into electrical energy. A suitable mathematical model that mimics the behaviour of the PV cell and precisely determines its parameter's optimal values is necessary for PV cells to operate well. These parameters are useful for assessing the consistency and accuracy of the models. The imbalanced operating scenarios, including malfunctions and ageing, make parameter evaluation difficult. The SD and DD mathematical models are the most popular and commonly used [5–7]. The SD model is used in the majority of situations due to its simplicity and acceptability.

Evaluating the PV parameters is a nonlinear, multidimensional problem that can be thought of as an optimisation problem. For extracting parameters from solar PV systems, stochastic methods called metaheuristics, which are inspired by nature, have proven to be an excellent replacement for traditional optimisation algorithms. A guided random search method deemed metaheuristic exploits and explores the entire search space. However, the solution is imperfect and could become stuck at a local optimum point. In the metaheuristic procedures, the quality of the solution and the time required to find it must typically be traded off. The quality of the solution must occasionally be compromised in order to reach a conclusion promptly [8–10].

A variety of techniques were developed and investigated to obtain more exact and precise parameters from nonlinear implicit equations with high precision. There are two primary types of algorithms listed in Table 1: metaheuristic and analytical. The hybrid chimp–sine cosine algorithm (HCSCA) [5], "enhanced hybrid grey wolf optimiser-sine cosine algorithm (EHGWOSCA)" [6], genetic algorithm [11], particle swarm optimisation [12], jellyfish search [13], hybrid differential evolution [14], cuckoo search with biogeography-based optimisation [15], pattern search [16], tunicate swarm [17], differential evolution [18], harmony search [19], tabu search [20], sooty tern [21], cat swarm [22], crow search [23], grey wolf optimiser [24], firefly algorithm [25], artificial bee colony [26], equilibrium optimiser [27], social spider algorithm [28], whale optimiser [29], humming bird optimiser [30], and bonobo optimiser [31] are examples of the metaheuristic algorithms. Analytical algorithms include "Lambert W-functions" [32], the conductivity method [33], least squares [34], the analytical mathematical method [35] and iterative method [36]. Analytical algorithms have limited applications due to the objective functions' persistence, uniqueness, and roundness. These algorithms are often sensitive to the initial solution and find local optima. Bio-related algorithms are more realistic and reliable optimisation approaches for simplifying complicated fundamental equations since they do not require challenging mathematics.

Table 1. A summary of metaheuristic and analytical techniques employed in the literature.

Reference	Algorithm	Analytical Method	Metaheuristic Method	Model
[5]	Hybrid chimp–sine cosine algorithm		√	SD and DD models
[6]	Enhanced hybrid grey wolf optimiser–sine cosine algorithm		√	SD and DD models
[11]	Genetic algorithm		√	DD model
[12]	Particle swarm optimisation		√	SD and DD models
[13]	Jellyfish search		√	SD model
[14]	Hybrid differential evolution		√	SD and DD models
[15]	Cuckoo search with biogeography-based optimisation		√	SD and DD models
[16]	Pattern search		√	SD and DD models
[17]	Tunicate swarm		√	SD model
[18]	Differential evolution		√	SD and DD models
[19]	Harmony search		√	SD and DD models
[20]	Tabu search		√	SD model
[21]	Sooty tern		√	SD model
[22]	Cat swarm		√	SD and DD models
[23]	Crow search		√	SD model
[24]	Gray wolf optimiser		√	SD and DD models
[25]	Firefly algorithm		√	SD and DD models
[26]	Artificial bee colony		√	SD and DD models
[27]	Equilibrium optimiser		√	SD and DD models
[28]	Social spider algorithm		√	SD and DD models
[29]	Whale optimiser		√	Triple diode (TD) model
[30]	Humming bird optimiser		√	TD model
[31]	Bonobo optimiser		√	SD and DD models
[32]	Lambert W-functions	√		DD model
[33]	Conductivity method	√		SD model
[34]	Least squares	√		SD model
[35]	Analytical mathematical method	√		SD model
[36]	Iterative method	√		SD model

Gong et al. [37] recently presented the dandelion algorithm in the framework of effective metaheuristic approaches. Based on it, two more dandelion algorithms were proposed, the variant dandelion algorithm [38] and DOA [39], to overcome the drawbacks of premature convergence and local optimisation.

In terms of high optimisation accuracy and effectiveness, DOA can replace the prior bio-inspired swarm intelligence OAs and produce superior convergence accuracy with less progressions. The main purposes of this study are as follows:

- In order to estimate the parameters of the PV modules, this work seeks to propose the novel bio-inspired swarm intelligence OA called the DOA for the first time.
- SD and DD approaches are used to mathematically model monocrystalline SF430M, polycrystalline SG350P, and thin-film Shell ST40 PV panels.
- The values of the practical dataset are taken into account while generating the error values and the objective function that would be used to reduce the error at various operational points.
- Utilizing the details from the datasheet on the three key components of a PV cell's *V*–*I* characteristic, an error function is suggested.
- All PV cell characteristics are optimised for SD and DD models without assuming any cell parameters.

2. PV Models

The output properties of the PV model may be correctly represented using a mathematical model. This will illustrate the biological functions that take place in the module's cell. The SD and DD models are the most commonly used ones. By assuming that the cells are equivalent and operate under comparable conditions, the parameters of the PV cell are extracted. This criterion is employed to create the objective functions for the model's description.

2.1. SD Model

Ideal PV and practical PV cells of SD model are shown in Figure 1. By using Kirchhoff's current law (KCL), the output current (I) is expressed in terms of the photocurrent (I_c), diode current (I_d), and shunt resistor current (I_{sh}):

$$I = I_c - I_d - I_{sh} \tag{1}$$

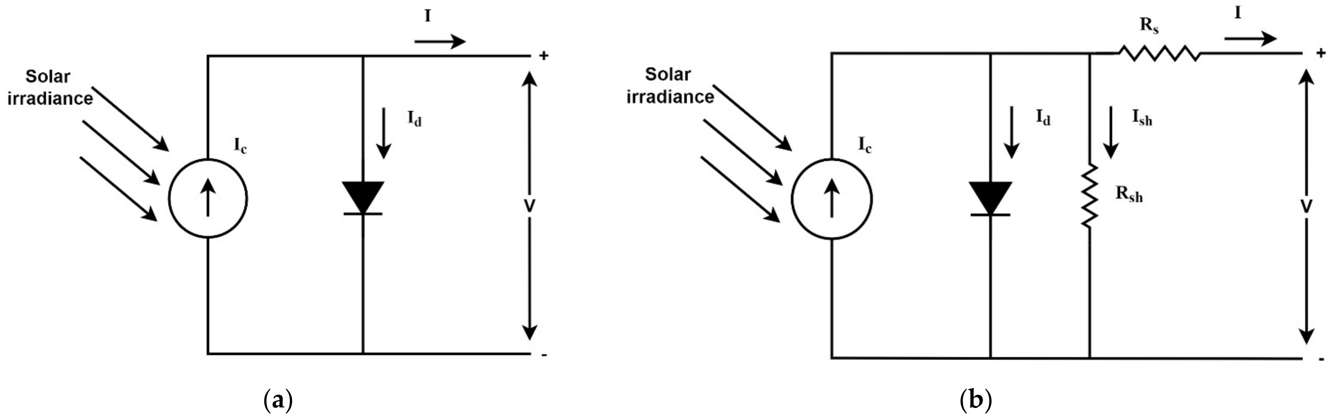

Figure 1. SD model of (**a**) ideal PV, and (**b**) practical PV cell.

The I_d and I_{sh} equations are represented by

$$I_d = I_s \left[e^{\left\{ \frac{q(V+IR_S)}{mKN\tau} \right\}} - 1 \right] \tag{2}$$

$$I_{sh} = \frac{V + IR_s}{R_{sh}} \tag{3}$$

By using Equations (2) and (3), Equation (1) is modified to

$$I = I_c - I_s\left[e^{\left\{\frac{q(V+IR_s)}{mKN\tau}\right\}} - 1\right] - \frac{V + IR_s}{R_{sh}} \tag{4}$$

where R_s and R_{sh} are the series and shunt resistances, I_s is the saturation current, m is the diode quality factor, V is the output voltage, τ stands for the p-n junction's temperature (in Kelvin), q stands for the electron charge, N represents the number of solar cells in series, and K stands for the Boltzmann constant.

Equation (4) shows that the SD model contains five parameters that must be extracted: I_c, I_s, R_s, R_{sh} and m.

Equation (4) is modified under open-circuit (OC) conditions $(I = 0; V = V_{oc})$ to

$$I_c = I_s\left[e^{\left\{\frac{qV_{oc}}{mKN\tau}\right\}} - 1\right] + \frac{V_{oc}}{R_{sh}} \tag{5}$$

Under short-circuit (SC) conditions $(V = 0; I = I_{sc})$, Equation (4) is modified to

$$I_c = I_{sc} + I_s\left[e^{\left\{\frac{qI_{sc}R_s}{mKN\tau}\right\}} - 1\right] + \frac{I_{sc}R_s}{R_{sh}} \tag{6}$$

I_s is expressed by using Equations (5) and (6) as

$$I_s = \frac{I_{sc} + \frac{I_{sc}R_s}{R_{sh}} - \frac{V_{oc}}{R_{sh}}}{e^{\left\{\frac{qV_{oc}}{mKN\tau}\right\}} - e^{\left\{\frac{qI_{sc}R_s}{mKN\tau}\right\}}} \tag{7}$$

Equation (4) is expressed at maximum power point (MPP) $(I = I_{MPP}; V = V_{MPP})$ as

$$I_{MPP} = I_c - I_s\left[e^{\left\{\frac{q(V_{MPP}+I_{MPP}R_s)}{mKN\tau}\right\}} - 1\right] - \frac{V_{MPP} + I_{MPP}R_s}{R_{sh}} \tag{8}$$

2.2. DD Model

The DD model with a second diode linked in parallel to the first is shown in Figure 2.

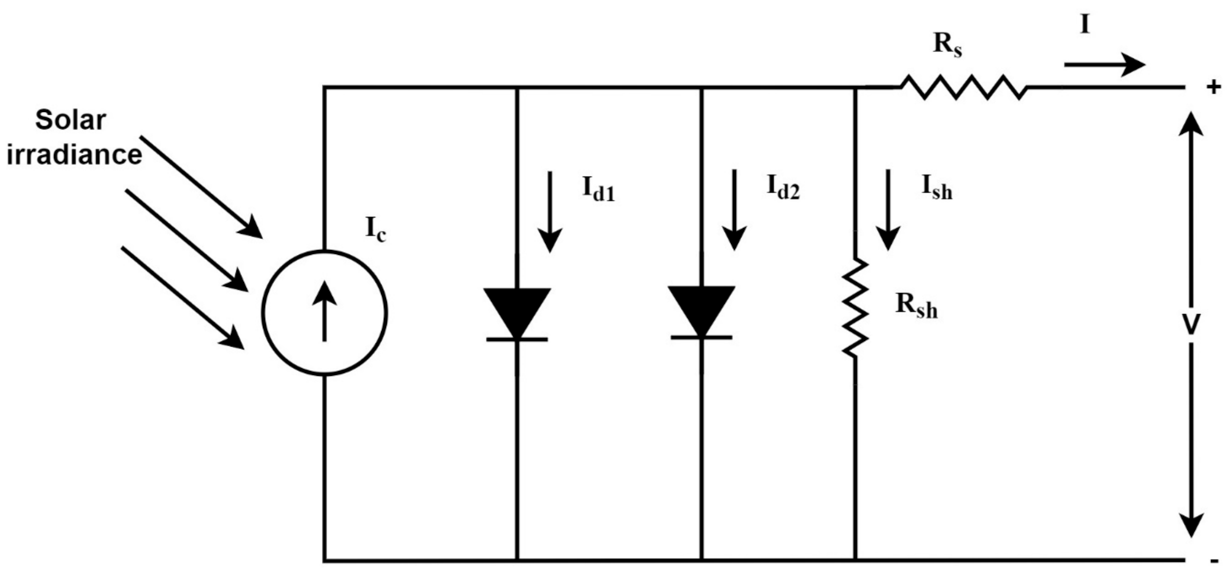

Figure 2. DD model of the PV cell.

By using KCL, the output current (I) is expressed as

$$I = I_c - I_{d1} - I_{d2} - I_{sh} \tag{9}$$

where I_{d1} and I_{d2} are the diode currents and they are represented in terms of saturation currents I_{s1} and I_{s2} and diode quality factors m_1 and m_2 by

$$I_{d1} = I_{s1}\left[e^{\left\{\frac{q(V+IR_s)}{m_1 KN\tau}\right\}} - 1\right] \tag{10}$$

$$I_{d2} = I_{s2}\left[e^{\left\{\frac{q(V+IR_s)}{m_2 KN\tau}\right\}} - 1\right] \tag{11}$$

By using Equations (3), (10) and (11), Equation (9) is modified to

$$I = I_c - I_{s1}\left[e^{\left\{\frac{q(V+IR_s)}{m_1 KN\tau}\right\}} - 1\right] - I_{s2}\left[e^{\left\{\frac{q(V+IR_s)}{m_2 KN\tau}\right\}} - 1\right] - \frac{V+IR_s}{R_{sh}} \tag{12}$$

Equation (12) shows that the DD model contains seven parameters that must be extracted: $I_c, I_{s1}, I_{s2}, R_s, R_{sh}, m_1$ and m_2.

Equation (12) is modified under OC conditions ($I = 0; V = V_{oc}$) to

$$I_c = I_{s1}\left[e^{\left\{\frac{qV_{oc}}{m_1 KN\tau}\right\}} - 1\right] + I_{s2}\left[e^{\left\{\frac{qV_{oc}}{m_2 KN\tau}\right\}} - 1\right] + \frac{V_{oc}}{R_{sh}} \tag{13}$$

Under SC conditions ($V = 0; I = I_{sc}$), Equation (12) is modified to

$$I_c = I_{sc} + I_{s1}\left[e^{\left\{\frac{qI_{sc}R_s}{m_1 KN\tau}\right\}} - 1\right] + I_{s2}\left[e^{\left\{\frac{qI_{sc}R_s}{m_2 KN\tau}\right\}} - 1\right] + \frac{I_{sc}R_s}{R_{sh}} \tag{14}$$

Equation (12) is expressed at the MPP ($I = I_{MPP}; V = V_{MPP}$) as

$$I_{MPP} = I_c - I_{s1}\left[e^{\left\{\frac{q(V_{MPP}+I_{MPP}R_s)}{m_1 KN\tau}\right\}} - 1\right] - I_{s2}\left[e^{\left\{\frac{q(V_{MPP}+I_{MPP}R_s)}{m_2 KN\tau}\right\}} - 1\right] - \frac{V_{MPP}+I_{MPP}R_s}{R_{sh}} \tag{15}$$

3. Dandelion Optimisation Algorithm

Recently, Zhao et al. [39] proposed a new bio-inspired swarm intelligence OA based on the flight modes of dandelion seeds (DSs) called the DOA. Dandelion is one of the plants that uses wind to spread its seeds. The two main parameters that influence the dispersal of dandelion seeds are wind velocity and climate. A seed's ability to fly long or short distances depends on the wind speed. The ability of DSs to fly and the likelihood that they will spread to neighbouring or distant areas are both influenced by the weather. The three phases that DSs go through are listed below.

- When a DS is in the rising stage, a vortex is created above it, and it rises due to a pulling force under windy and bright conditions. In contrast, when it is raining, no eddies are above the seeds. In this situation, only local searches are possible.
- In the landing stage, DSs finally randomly settle in one location under the influence of wind and weather to create new dandelions.
- In the descending stage, once seeds soar up to a given height, they drop continuously.

Dandelions evolve their population by dispersing their seeds to the next generation in three stages.

3.1. Mathematical Formulation of the DOA

This part discusses the mathematical formulas for the DOA. The mathematical formulas for the rising stage with the two types of weather circumstances are presented first, and then the descending stage and landing stage mathematical formulas are examined [39].

3.1.1. Rising Stage

In the DOA, the assumption is made that each DS corresponds to a potential solution and its population is given by

$$population = \begin{bmatrix} \chi_1^1 & \cdots & \chi_1^{dm} \\ \vdots & \ddots & \vdots \\ \chi_{pp}^1 & \cdots & \chi_{pp}^{dm} \end{bmatrix} \quad (16)$$

where pp is the size of the population, and dm is the variable dimension.

The individual position X_j is defined as

$$X_j = r_1(UPB - LOB) + LOB \quad (17)$$

where $j = 1, 2, 3, \ldots, pp$; r_1 is the arbitrary number between 0 and 1; UPB is the upper bound; LOB is the lower bound of the given problem and is represented as

$$UPB = [upb_1, \cdots, upb_{dm}],\ LOB = [lob_1, \cdots, lob_{dm}] \quad (18)$$

At the time of initialisation, the DOA considers the individual with the highest fitness value to be the first elite, which is roughly regarded as the best situation for the DS to grow. By using the minimum value as an illustration, the equation of the first elite, X_{elite}, is given by

$$f_{best} = min(f(X_j)), X_{elite} = X(find(f_{best} == f(X_j))) \quad (19)$$

where *find*( ) refers to two equal-value indices.

DSs in the rising stage must reach a particular height so that they can float apart from their mother plant. DSs rise to various heights depending on the wind velocity, air moisture, etc.

Here, two types if weather circumstances are considered.

Case 1. Wind velocities on a sunny day may be thought of as having a lognormal distribution, $\ln \mathrm{Y} \sim N(\mu, \sigma^2)$. In this case, DSs are dispersed arbitrarily by the wind in the search space. The wind speed affects how high a DS will rise. The higher the dandelion flies and the further the seeds are dispersed, the stronger the wind is. The wind speed changes the vortexes above the DSs, causing them to ascend in a spiral shape.

In this instance, the relevant mathematical expression is

$$X_{t+1} = X_t + \alpha * \vartheta_x * \vartheta_y * \ln \mathrm{Y} * (X_{rs} - X_t) \quad (20)$$

where X_t denotes the position of DS when iteration t begins. The location in the search space that is arbitrarily chosen during iteration t is represented by X_{rs}. The formula for the location that is created arbitrarily is given by

$$X_{rs} = r_1(1, dm) * (UPB - LOB) + LOB \quad (21)$$

The mathematical expression for the lognormal distribution $\ln \mathrm{Y}$, where $\mu = 0$ and $\sigma^2 = 1$, is

$$\ln \mathrm{Y} = \begin{cases} \frac{1}{y\sqrt{2\pi}} exp\left[\frac{-1}{2\sigma^2}(\ln y)^2\right] & y \geq 0 \\ 0 & y < 0 \end{cases} \quad (22)$$

where y stands for the standard normal distribution, $N(0,1)$, and α stands for the adaptive parameter used to modify the search step length, and its expression is

$$\alpha = r_1 * \left(\frac{1}{T^2}t^2 - \frac{2}{T}t + 1\right) \tag{23}$$

The lift component factors of a dandelion caused by the separated eddy action are represented by ϑ_x and ϑ_y. To determine the force acting on the variable dimension, use Equation (24) as a guide.

$$r = \frac{1}{e^\theta},\ \vartheta_x = r * cos\theta,\ \vartheta_y = r * sin\theta \tag{24}$$

where θ is the arbitrary number between $[-\pi, \pi]$.

Case 2. DSs struggle to rise properly with the wind on rainy days due to air resistance, humidity, and other reasons. Since DSs are being used in this situation in the local community, the relevant mathematical equation is

$$X_{t+1} = X_t * k \tag{25}$$

where k controls the dandelion's local search domain and the domain's size (ϱ) is determined using Equation (26)

$$\varrho = \frac{1}{T^2 - 2T + 1}t^2 - \frac{2}{T^2 - 2T + 1}t + \frac{1}{T^2 - 2T + 1},\ k = 1 - rand() * \varrho \tag{26}$$

Finally, the mathematical representation of DSs in rising stage is

$$X_{t+1} = \begin{cases} X_t + \alpha * \vartheta_x * \vartheta_y * \ln Y * (X_{rs} - X_t) & randn < 1.5 \\ X_t * k & else \end{cases} \tag{27}$$

where T is the maximum number of iterations and $randn()$ is the arbitrary value that follows the standard normal distribution.

3.1.2. Descending Stage

The DOA likewise places a strong emphasis on exploration at this step. DSs rise up to a given distance and then slowly begin to drop. Brownian motion is used in the DOA to mimic the path of a dandelion as it moves. In the process of iterative updating, it is simple for the individual to go through additional search communities since Brownian motion follows a normal distribution with each update. The average position data after the rising stage are used to indicate the steadiness of the dandelion's fall. This encourages the population's overall growth toward promising conditions.

The mathematical representation of DSs in the descending stage is

$$X_{t+1} = X_t - \alpha * \beta_t * (X_{mean-t} - \alpha * \beta_t * X_t) \tag{28}$$

where β_t is the Brownian motion and it is an arbitrary number from the standard normal distribution, and X_{mean-t} is population's average position in the jth iteration; its equation is

$$X_{mean-t} = \frac{1}{pp}\sum_{j=1}^{pp} X_j \tag{29}$$

3.1.3. Landing Stage

The DOA concentrates on exploitation in this section. The DS chooses where to fall at random based on the previous two steps. Hopefully, the algorithm reaches the global optimal solution as the iterations advance gradually. The optimal option is the approximate location where dandelion seeds would survive most easily. Search agents use the expert knowledge of the current elite to their advantage in their local communities in order to precisely converge to the global optimum. Eventually, population evolution leads to the discovery of the global optimal solution. The mathematical representation of DSs in the landing stage is

$$X_{t+1} = X_{elite} + levy(\lambda) * \alpha * (X_{elite} - X_t * \delta) \tag{30}$$

where X_{elite} denotes the DSs' optimal placement in the jth iteration, $\delta = \frac{2t}{T}$, and $levy(\lambda)$ is the function of Levy flight; its expression is

$$levy(\lambda) = s * \frac{\omega * \sigma}{|t|^{1/\beta}} \tag{31}$$

where $\beta = 1.5$, $s = 0.01$, ω and t are the arbitrary numbers between $[0, 1]$, and $\sigma = \left[\frac{\Gamma(1+\beta) * sin\left(\frac{\pi\beta}{2}\right)}{\Gamma\left(\frac{1+\beta}{2}\right) * \beta * 2^{\left(\frac{\beta-1}{2}\right)}} \right]$.

A pseudo code [39] and flow chart of the DOA is given in Table 2 and Figure 3, respectively.

Table 2. Pseudo code of DOA.

Pseudo Code of DOA

Input variables: pp, dm, T.
Output variables: Optimal DS X_{best} and its fitness value, f_{best}.
Initialise DSs' X of the DOA
Determine each DSs' fitness value, f.
Choose the optimum DS X_{elite} based on fitness values.
while $(t < T)$ **carry out**
/*Rising stage*/
if $randn() < 1.5$ **carry out**
By using Equation (23), produce adaptive parameters.
By using Equation (20), update DSs.
otherwise, carry out
By using Equation (26), produce adaptive parameters.
By using Equation (25), update DSs.
end if
/*Declining stage*/
By using Equation (28), update DSs.
/*Landing stage*/
By using Equation (30), update DSs.
Arrange DSs in a fitness value-based hierarchy of good to bad.
Update X_{elite}
if $f(X_{elite}) < f(X_{best})$
$X_{best} = X_{elite}$, $f_{best} = f(X_{elite})$
end if
end while
Return X_{best} and f_{best}.

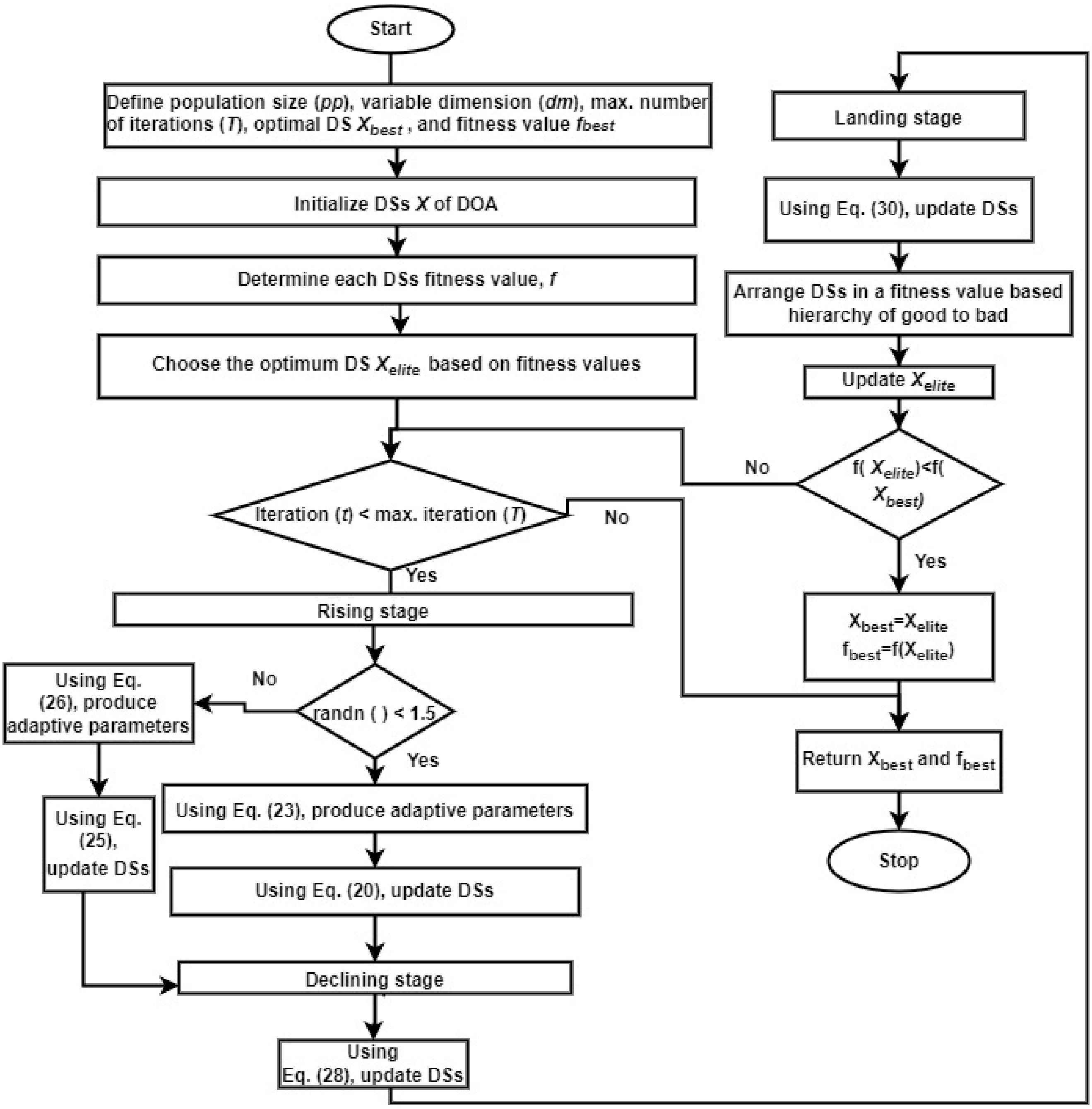

Figure 3. Flow chart representation of DOA algorithm.

4. Formulation of the Optimisation Problem

The objective of PV module parameter estimation is the accurate estimation of the *V*–*I* characteristics. The majority of publications just aim for MPP accuracy. SC, OC, and MPP are the three points that this paper mainly concentrates on. It is important to reduce errors at these three locations. The total of the squares of the three errors is the net error and the proposed optimisation algorithm is designed to reduce this error [18,23,24,27].

In the case of the SD model, the error at the OC point is

$$\epsilon_{oc} = I_s\left[e^{\left\{\frac{qV_{oc}}{mKN\tau}\right\}} - 1\right] + \frac{V_{oc}}{R_{sh}} - I_c \tag{32}$$

The error at the SC point is

$$\epsilon_{sc} = I_{sc} + I_s\left[e^{\left\{\frac{qI_{sc}R_s}{mKN\tau}\right\}} - 1\right] + \frac{I_{sc}R_s}{R_{sh}} - I_c \tag{33}$$

The error at the MPP is

$$\epsilon_{MPP} = I_c - I_s\left[e^{\left\{\frac{q(V_{MPP}+I_{MPP}R_s)}{mKN\tau}\right\}} - 1\right] - \frac{V_{MPP} + I_{MPP}R_s}{R_{sh}} - I_{MPP} \tag{34}$$

The net error is

$$\epsilon = \epsilon_{oc}^2 + \epsilon_{sc}^2 + \epsilon_{MPP}^2 \tag{35}$$

In the case of the DD model, the error at the OC point is

$$\epsilon_{oc} = I_{s1}\left[e^{\left\{\frac{qV_{oc}}{m_1KN\tau}\right\}} - 1\right] + I_{s2}\left[e^{\left\{\frac{qV_{oc}}{m_2KN\tau}\right\}} - 1\right] + \frac{V_{oc}}{R_{sh}} - I_c \tag{36}$$

The error at the h point is

$$\epsilon_{sc} = I_{sc} + I_{s1}\left[e^{\left\{\frac{qI_{sc}R_s}{m_1KN\tau}\right\}} - 1\right] + I_{s2}\left[e^{\left\{\frac{qI_{sc}R_s}{m_2KN\tau}\right\}} - 1\right] + \frac{I_{sc}R_s}{R_{sh}} - I_c \tag{37}$$

The error at the MPP is

$$\epsilon_{MPP} = I_c - I_{s1}\left[e^{\left\{\frac{q(V_{MPP}+I_{MPP}R_s)}{m_1KN\tau}\right\}} - 1\right] - I_{s2}\left[e^{\left\{\frac{q(V_{MPP}+I_{MPP}R_s)}{m_2KN\tau}\right\}} - 1\right] - \frac{V_{MPP} + I_{MPP}R_s}{R_{sh}} - I_{MPP} \tag{38}$$

The net error is

$$\epsilon = \epsilon_{oc}^2 + \epsilon_{sc}^2 + \epsilon_{MPP}^2 \tag{39}$$

5. Procedural Steps for PV Module Parameter Estimation

The following are the steps that describe how to calculate solar PV module parameters using the applied algorithm:

Step 1: Initialise the variables for the solar PV module and the algorithm as described in Tables 2–4.
Step 2: Verify the maximum iteration count before moving on to the next stages. If not, go to step 7.
Step 3: Utilizing Equations (1)–(15), take into account the SD and DD models for the solar PV module under consideration.
Step 4: Use Equations (16)–(31) to implement the suggested DOA for the research subject under consideration.
Step 5: Reduce the net error given by Equations (35) and (39) for steps 3 and 4 for each iteration.
Step 6: Count up the iterations and go on to step 2.
Step 7: Completely analyse various solar PV modules and determine the best values for equivalent circuit parameters.

6. Results and Analysis

Using SD and DD models, the current magnitudes under various operating situations have been mathematically modelled. The producers of the PV modules offer the actual data for these values for each PV model variant. To illustrate the effectiveness of the suggested DOA, monocrystalline SF430M, polycrystalline SG350P, and thin-film Shell ST40 panels are taken into consideration. By comparing the values of the mathematical model and the data set, the error magnitude is determined. The DOA is used in this paper to reduce the overall error. The DOA evaluates 30 search agents across 500 iterations using a MATLAB environment. The following SD and DD models are used to illustrate the effectiveness of the entire system. Datasheet parameters of various PV panels are given by Table 3 and parameter constraints of SD and DD models are given by Table 4.

Table 3. Datasheet parameters of various PV panels.

	Monocrystalline SF430M [40]	Polycrystalline SG350P [41]	Thin Film Shell ST40 [42]
V_{MPP}	41.2 V	38.7 V	16.60 V
I_{MPP}	10.44 A	9.05 A	2.41 A
V_{oc}	49.4 V	47.22 V	23.30 V
I_{sc}	11.06 A	9.68 A	2.68 A
Temperature coefficient of P_{max}	−0.37%/°C	−0.39%/°C	−0.6%/°C
Temperature coefficient of V_{oc}	−0.28%/°C	−0.28%/°C	−0.1%/°C
Temperature coefficient of I_{sc}	0.042%/°C	0.042%/°C	0.00035%/°C
N	72	72	36

Table 4. Parameter constraints of SD and DD models.

SD Model	DD Model	UPB	LOB
m	m_1, m_2	2	0.5
R_s (Ω)		1	0.001
R_{sh} (Ω)		200	50
-	$I_{s1}(A)$	10^{-6}	10^{-12}

6.1. Parameter Estimation for SD Model of Various PV Panels

Monocrystalline SF430M, polycrystalline SG350P and thin-film Shell ST40 PV panels are used for parameter estimation. Tables 5–7 list the SD model's optimal parameters throughout 30 runs, and Figures 4–6 display the simulation's findings. Out of five parameters in the SD model, three (m, R_s, R_{sh}) are optimised using the DOA, whereas the other two (I_c, I_s) are derived using the resulting analytical equations.

Table 5. SD model of monocrystalline SF430M PV panel's optimal estimated parameters using DOA and analytical method.

Run	DOA			Analytical Method		Error (ϵ)
	m	R_s (Ω)	R_{sh} (Ω)	I_s (A)	I_c (A)	
1	0.5066	0.1687	67.4524	1.3264e-22	11.0876	2.0477e-17
2	1.2660	0.0490	192.0358	7.4668e-09	11.0628	3.2914e-16
3	0.8881	0.2720	200	9.4742e-13	11.0750	1.1424e-15
4	0.5713	0.0039	66.9424	5.1739e-20	11.0606	1.3270e-16
5	1.3555	0.0018	199.9999	3.0059e-08	11.0601	7.2251e-18
6	0.6542	0.0016	67.7582	1.9423e-17	11.0602	4.3208e-19
7	0.5034	0.1197	66.9729	9.4619e-23	11.0797	1.5614e-17
8	0.5002	0.0368	66.6534	6.7940e-23	11.0661	2.1375e-16
9	0.5371	0.0010	66.7436	2.6568e-21	11.0601	7.8490e-17
10	1.3274	0.0010	174.4444	1.9764e-08	11.0600	3.6750e-16
11	0.7852	0.2784	120.3921	1.8180e-14	11.0855	5.1414e-16
12	1.2109	0.0278	134.2327	2.8318e-09	11.0622	3.2215e-16
13	1.2172	0.0599	166.3733	3.1930e-09	11.0639	7.9023e-16
14	1.2826	0.0012	147.3545	9.7396e-09	11.0600	2.2499e-17
15	0.7910	0.2354	99.9845	2.3137e-14	11.0860	5.7332e-16
16	0.7712	0.1772	82.5875	9.6369e-15	11.0837	3.6795e-16
17	0.7539	0.3495	199.5575	4.4962e-15	11.0793	6.0320e-15
18	0.5042	0.3379	74.4950	1.0425e-22	11.1101	1.3074e-16
19	1.0320	0.0311	91.5428	6.0852e-11	11.0637	7.1674e-18
20	0.7755	0.3104	145.9505	1.1957e-14	11.0835	8.2083e-17
21	0.5258	0.3054	73.2910	9.2226e-22	11.1060	2.7147e-16
22	1.1985	0.0324	132.1643	2.2530e-09	11.0627	7.9011e-16
23	1.1650	0.0010	107.6268	1.1776e-09	11.0601	6.5412e-16

Table 5. *Cont.*

Run	DOA			Analytical Method		Error (ϵ)
	m	R_s (Ω)	R_{sh} (Ω)	I_s (A)	I_c (A)	
24	1.3158	0.0242	199.0640	1.6608e-08	11.0613	1.0871e-17
25	0.6172	0.4012	136.4209	1.7383e-18	11.0925	4.7216e-15
26	1.3098	0.0281	199.9976	1.5139e-08	11.0615	1.2625e-15
27	1.3465	0.0053	197.1366	2.6373e-08	11.0602	8.4918e-18
28	1.0055	0.0010	83.7745	3.0648e-11	11.0601	2.5118e-19
29	1.3087	0.0277	197.9710	1.4874e-08	11.0615	6.2800e-18
30	0.8707	0.0011	74.1570	4.9832e-13	11.0601	9.2189e-16

Table 6. SD model of polycrystalline SG350P PV panel's optimal estimated parameters using DOA and analytical method.

Run	DOA			Analytical Method		Error (ϵ)
	m	R_s (Ω)	R_{sh} (Ω)	I_s (A)	I_c (A)	
1	1.1646	0.2096	199.9853	2.8627e-09	9.6901	1.4939e-15
2	1.1653	0.0330	90.4115	2.8122e-09	9.6835	9.3348e-17
3	0.6375	0.5293	166.0917	3.8465e-17	9.7108	4.7089e-16
4	0.5844	0.3777	70.0374	9.7381e-19	9.7322	2.9725e-17
5	0.9470	0.3123	144.4529	1.8440e-11	9.7009	1.3180e-16
6	1.2380	0.0372	104.2750	1.0256e-08	9.6834	6.6337e-17
7	0.7656	0.0010	63.6454	2.9652e-14	9.6801	1.3493e-15
8	1.2212	0.0449	102.9439	7.7210e-09	9.6842	3.9785e-17
9	0.5007	0.5712	100.5910	6.7232e-22	9.7349	1.3128e-17
10	0.5058	0.0089	61.5251	1.0856e-21	9.6814	8.6616e-18
11	1.3712	0.0634	176.1996	7.7475e-08	9.6834	3.5573e-16
12	0.8829	0.0219	67.2878	2.5012e-12	9.6831	9.4824e-21
13	0.5839	0.5035	97.3535	9.5643e-19	9.7300	3.8534e-15
14	0.9045	0.2719	100.6567	5.1312e-12	9.7061	2.9987e-19
15	0.5000	0.1212	61.5931	6.0347e-22	9.6990	2.7429e-18
16	0.5482	0.3212	64.7611	5.4297e-20	9.7280	2.9782e-17
17	1.2184	0.1745	197.5454	7.5298e-09	9.6885	2.0915e-18
18	1.2666	0.0027	100.5927	1.6296e-08	9.6802	2.5461e-16
19	0.9359	0.3406	173.1933	1.3469e-11	9.6990	8.7728e-17
20	0.8806	0.0233	67.2490	2.3198e-12	9.6833	5.1891e-18
21	1.2004	0.0526	100.7845	5.3659e-09	9.6850	2.9264e-16
22	0.7652	0.0023	63.6575	2.9201e-14	9.6803	7.3543e-16
23	1.4965	0.0010	199.9981	3.6934e-07	9.6800	1.1224e-16
24	0.5805	0.3121	65.8014	7.2393e-19	9.7259	2.9825e-16
25	0.5083	0.5426	88.8710	1.4328e-21	9.7391	5.9047e-16
26	0.6885	0.0087	62.5949	7.1022e-16	9.6813	3.4635e-17
27	1.3219	0.0081	114.8555	3.8116e-08	9.6806	1.8545e-15
28	1.3854	0.0081	136.1256	9.2943e-08	9.6805	3.9759e-19
29	0.5000	0.5914	117.5315	6.3105e-22	9.7287	1.1503e-15
30	1.3227	0.0089	115.4072	3.8580e-08	9.6807	3.4042e-17

Table 7. SD model of thin-film Shell ST40 PV panel's optimal estimated parameters using DOA and analytical method.

Run	DOA			Analytical Method		Error (ϵ)
	m	R_s (Ω)	R_{sh} (Ω)	I_s (A)	I_c (A)	
1	0.8755	0.0196	61.6039	7.3527e-13	2.6808	6.7055e-17
2	1.9964	0.2813	93.6305	8.0806e-06	2.6880	3.6331e-19
3	1.2467	0.0010	63.1023	3.8777e-09	2.6800	1.7621e-20
4	1.9999	0.5795	129.3084	8.5035e-06	2.6920	1.2099e-18

Table 7. *Cont.*

Run	DOA			Analytical Method		Error (ϵ)
	m	R_s (Ω)	R_{sh} (Ω)	I_s (A)	I_c (A)	
5	1.3212	0.7201	71.6375	1.2499e-08	2.7069	1.9623e-17
6	1.5900	0.5486	79.1210	3.1651e-07	2.6985	3.4663e-17
7	1.9994	0.2500	91.8552	8.2144e-06	2.6872	1.4853e-17
8	2	0.6332	141.8301	8.5618e-06	2.6919	9.1611e-19
9	1.2218	0.6531	67.1147	2.6236e-09	2.7060	9.8823e-18
10	1.3678	0.4519	68.0710	2.3658e-08	2.6977	7.7787e-18
11	0.9102	0.0544	61.6420	2.2034e-12	2.6823	1.1614e-17
12	1.8124	0.9591	199.1073	2.3699e-06	2.6929	8.5869e-17
13	1.9999	0.0010	80.5765	8.0980e-06	2.6800	5.0441e-18
14	1.0698	0.9999	68.3693	1.4132e-10	2.7191	2.4169e-19
15	0.5010	1	60.5315	3.4096e-22	2.7242	4.8679e-16
16	2	0.0010	80.5767	8.0983e-06	2.6800	1.7172e-16
17	0.5341	0.6183	60.8769	7.6567e-21	2.7072	9.2716e-17
18	1.6829	0.9989	150.2686	8.0317e-07	2.6978	1.0543e-18
19	0.5006	0.0010	61.4807	3.2193e-22	2.6800	2.8472e-18
20	1.9993	0.0010	80.5456	8.0632e-06	2.6800	7.4597e-20
21	1.9999	0.1435	86.1606	8.1721e-06	2.6844	2.7141e-19
22	1.6548	0.9116	118.6317	6.1330e-07	2.7005	2.3453e-16
23	1.9992	0.3316	97.5556	8.2591e-06	2.6891	6.2520e-17
24	1.3149	0.3712	65.9451	1.1203e-08	2.6950	2.0376e-18
25	1.5301	0.7428	84.3621	1.7192e-07	2.7035	4.3950e-17
26	2	0.2850	94.1917	8.2672e-06	2.6881	4.9402e-18
27	1.9999	0.6453	145.1735	8.5738e-06	2.6919	1.2349e-17
28	1.4116	0.9999	91.6732	4.3676e-08	2.7092	6.4730e-17
29	1.5287	0.9777	105.4428	1.7321e-07	2.7048	3.5642e-18
30	1.9999	0.5789	129.1812	8.5042e-06	2.6920	3.5939e-17

(**a**)

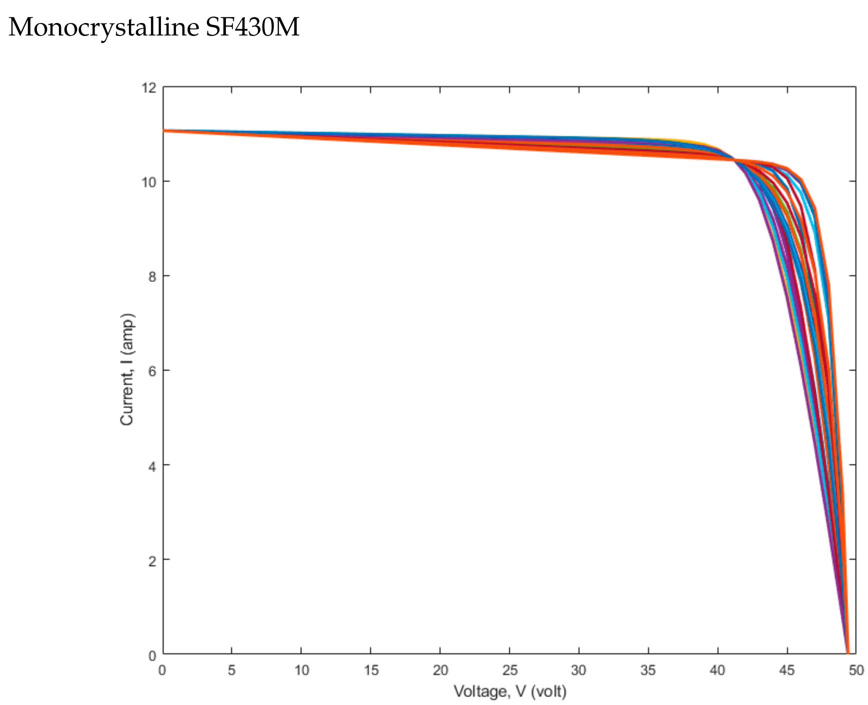

Figure 4. *Cont.*

(**b**)

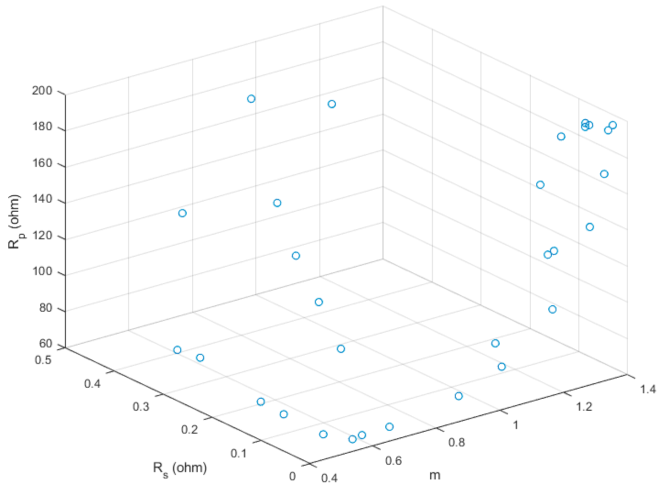

(**c**)

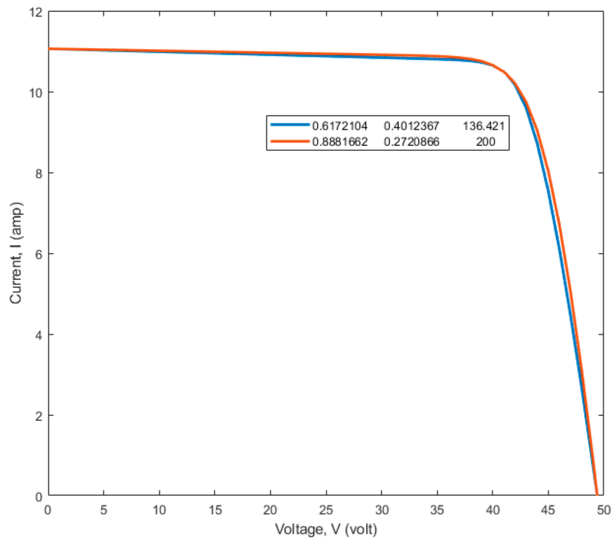

Figure 4. Simulation findings of parameter extraction of SD with monocrystalline SF430M PV panel's (**a**) *V–I* characteristics, (**b**) optimal solution set, and (**c**) *V–I* characteristics with maximum R_s and R_{sh}.

Polycrystalline SG350P

(**a**)

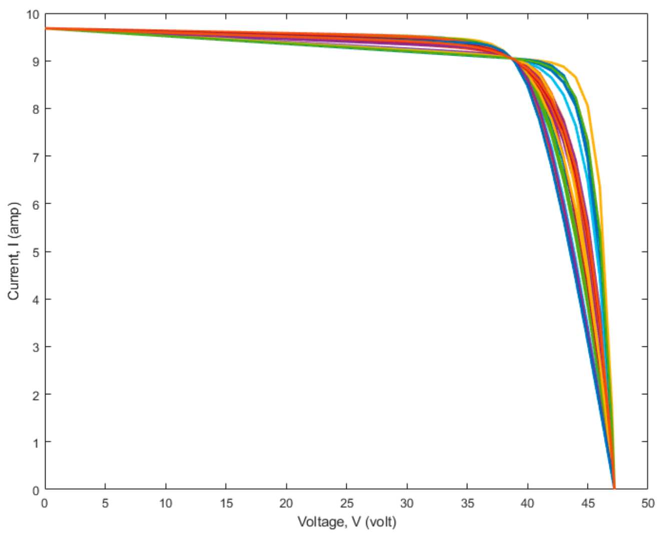

Figure 5. *Cont.*

(**b**)

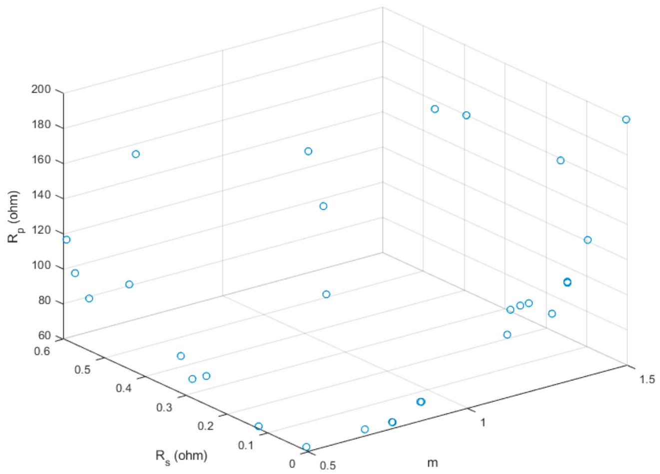

(**c**)

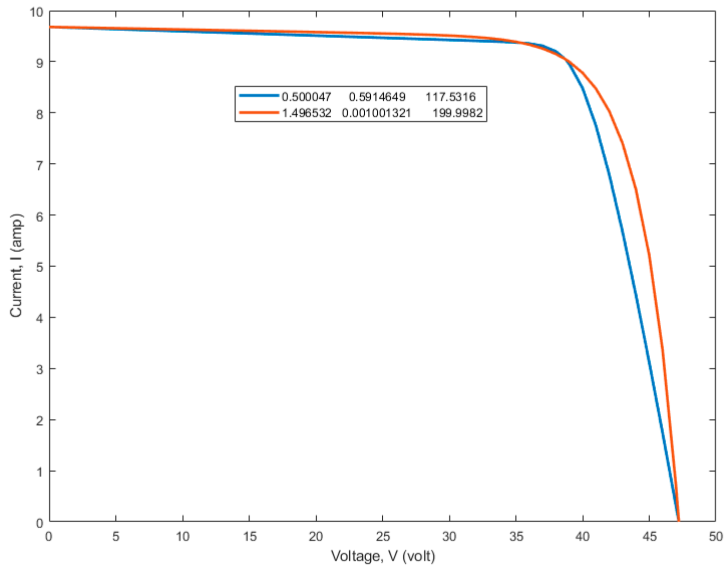

Figure 5. Simulation findings of parameter extraction of SD with Polycrystalline SG350P PV panel's (**a**) *V*–*I* characteristics, (**b**) optimal solution set, and (**c**) *V*–*I* characteristics with maximum R_s and R_{sh}.

Thin film Shell ST40 PV

(**a**)

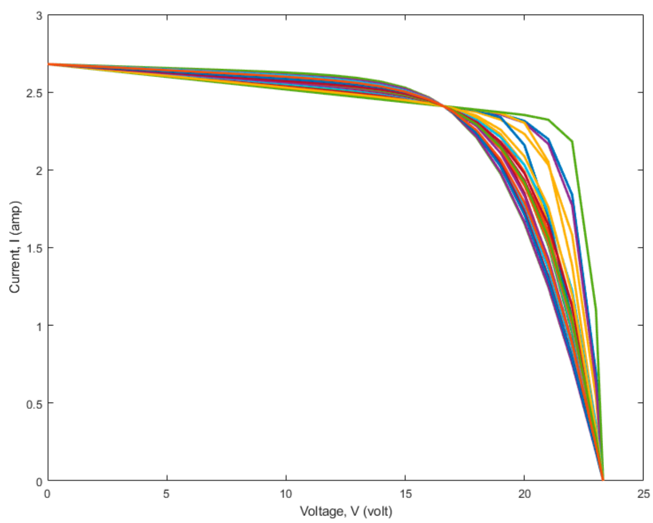

Figure 6. *Cont.*

(**b**)

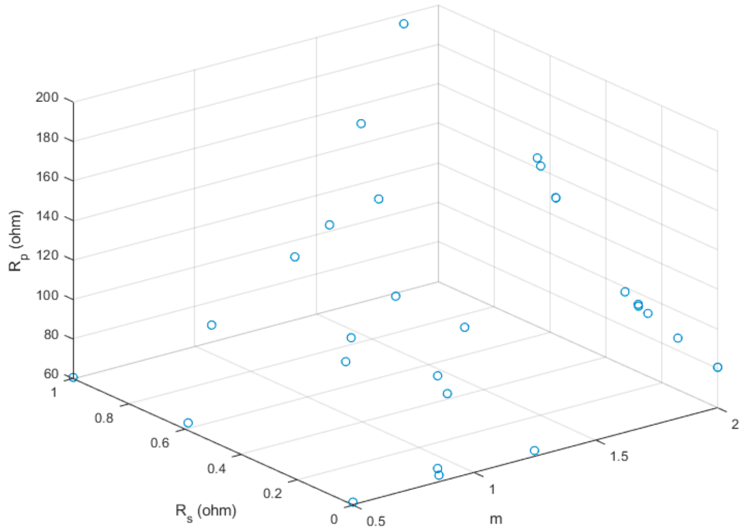

(**c**)

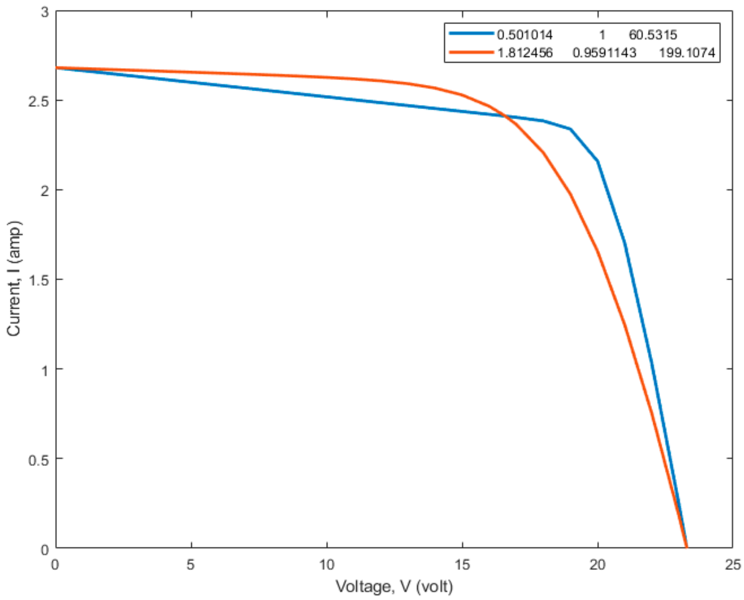

Figure 6. Simulation findings of parameter extraction of SD with thin-film Shell ST40PV panel's (**a**) *V*–*I* characteristics, (**b**) optimal solution set, and (**c**) *V*–*I* characteristics with maximum R_s and R_{sh}.

6.2. Parameter Estimation for DD Model of Various PV Panels

For parameter estimation of the DD model, monocrystalline SF430M, polycrystalline SG350P, and thin film Shell ST40 PV panels are taken into consideration. Tables 8–10 list the various PV module parameters for the DD model that were taken from 30 runs, and Figures 7–9 show the simulation results. Two parameters are determined analytically and five parameters are optimised using the DOA method in the DD model of the monocrystalline SF430M, polycrystalline SG350P and thin-film Shell ST40 PV panels.

Table 8. DD model of monocrystalline SF430M PV panel's optimal estimated parameters using DOA and analytical method.

Run	DOA				Analytical Method			Error (ϵ)
	m_1	m_2	R_s (Ω)	R_{sh} (Ω)	I_{s1} (A)	I_{s2} (A)	I_c (A)	
1	1.9995	0.5011	0.2134	85.7834	9.9900e-07	7.1045e-23	11.0875	1.3680e-19
2	1.9941	0.9350	0.2368	200	1.7376e-07	4.2362e-12	11.0730	3.5206e-19

Table 8. *Cont.*

Run	DOA				Analytical Method			Error (ϵ)
	m_1	m_2	R_s (Ω)	R_{sh} (Ω)	I_{s1} (A)	I_{s2} (A)	I_c (A)	
3	1.9990	0.9463	0.0170	88.6811	7.2968e-07	5.5871e-12	11.0621	1.6737e-19
4	1.9831	0.7116	0.0507	73.0153	3.0009e-07	5.1353e-16	11.0676	2.0463e-22
5	1.9705	1.0186	0.1882	187.9229	5.5469e-08	4.4296e-11	11.0710	8.8287e-19
6	1.9999	0.6093	0.3803	176.9380	7.2569e-07	9.5962e-19	11.0837	1.6842e-16
7	0.9387	0.9433	0.0219	80.4309	1.0000e-12	4.1537e-12	11.0630	2.9206e-16
8	1.7637	0.5832	0.3348	84.4166	1.0000e-12	1.3681e-19	11.1038	3.2421e-16
9	2	0.5183	0.1934	81.9717	8.7052e-07	4.1912e-22	11.0861	1.7695e-16
10	1.9474	0.9676	0.0086	88.5960	4.9116e-07	1.0402e-11	11.0610	8.2954e-16
11	1.9990	0.5264	0.1129	78.6888	9.4928e-07	9.1653e-22	11.0758	2.9086e-17
12	1.9874	1.3112	0.0010	164.3995	3.3751e-08	1.5345e-08	11.0600	4.7554e-18
13	1.7323	1.0026	0.0751	127.0942	2.5112e-07	2.5595e-11	11.0665	1.8711e-16
14	1.7614	0.6797	0.0010	68.1359	2.0044e-12	8.9493e-17	11.0601	1.0901e-16
15	2	0.6713	0.0015	68.0090	1.0088e-12	5.4977e-17	11.0602	1.0573e-16
16	1.3563	0.5015	0.0598	66.7099	1.0826e-12	7.7550e-23	11.0699	3.8492e-16
17	1.8579	0.6638	0.1562	123.6696	9.4765e-07	3.0473e-17	11.0739	6.8046e-17
18	1.8319	0.9528	0.2162	197.7403	1.3632e-07	7.0970e-12	11.0720	4.6200e-17
19	1.6426	0.9898	0.0255	90.0449	3.5376e-08	1.9408e-11	11.0631	1.5991e-16
20	1.6029	0.5095	0.0526	107.4908	1.8031e-07	1.2991e-22	11.0654	4.1592e-15
21	1.8880	1.1372	0.0525	165.7020	7.4178e-07	6.1687e-10	11.0635	1.7752e-15
22	1.8109	1.2843	0.0065	187.9730	3.4398e-07	9.2667e-09	11.0603	5.5379e-16
23	1.9597	0.5000	0.0047	66.6119	1.0438e-12	6.5820e-23	11.0607	1.9587e-17
24	1.8886	0.7354	0.0353	86.8116	7.8832e-07	1.5982e-15	11.0645	3.0808e-17
25	2	1.1299	0.1322	200	1.5061e-10	5.8883e-10	11.0673	2.6998e-16
26	1.1637	1.1580	0.1035	177.9818	4.4891e-12	1.0385e-09	11.0664	2.1860e-17
27	1.9179	0.5033	0.0934	70.0183	1.9303e-07	9.2160e-23	11.0747	4.6731e-19
28	1.9962	1.1017	0.0743	139.7824	6.4939e-07	3.0600e-10	11.0658	3.5561e-17
29	1.9077	0.5204	0.3728	133.9937	5.6407e-07	5.2070e-22	11.0907	5.5428e-16
30	1.9965	1.1041	0.0468	109.3303	1.0491e-12	3.3271e-10	11.0647	3.5995e-17

Table 9. DD model of polycrystalline SG350P PV panel's optimal estimated parameters using DOA and analytical method.

Run	DOA				Analytical Method			Error (ϵ)
	m_1	m_2	R_s (Ω)	R_{sh} (Ω)	I_{s1} (A)	I_{s2} (A)	I_c (A)	
1	1.6576	1.1248	0.0069	81.6958	1.0000e-12	1.2698e-09	9.6808	2.8303e-20
2	1.9906	0.8543	0.2141	83.0836	4.2553e-07	9.4815e-13	9.7049	5.1853e-17
3	1.9991	1.4048	0.0448	199.1375	8.2938e-07	1.1759e-07	9.6821	3.6797e-16
4	1.9748	0.5000	0.3272	65.7817	2.5592e-07	5.9983e-22	9.7281	3.5763e-18
5	1.9064	0.5879	0.0019	61.7913	2.2285e-09	1.2414e-18	9.6802	4.8951e-17
6	1.9998	0.7282	0.1379	68.0113	4.5339e-07	5.2963e-15	9.6996	2.8251e-16
7	1.9999	1.0190	0.1063	83.1975	2.2911e-10	1.2078e-10	9.6923	1.4634e-15
8	1.5716	1.4399	0.0010	157.4846	5.6125e-10	1.8746e-07	9.6800	2.1316e-15
9	1.8653	0.6441	0.5353	197.3307	8.8741e-09	5.8293e-17	9.7062	7.2147e-16
10	1.9704	0.6267	0.4949	111.2720	1.4728e-11	1.9082e-17	9.7230	7.2748e-16
11	1.6477	0.7135	0.3122	114.7205	2.2562e-07	2.3532e-15	9.7063	4.9865e-16
12	1.7373	1.3321	0.0551	199.8697	6.8321e-07	3.7210e-08	9.6826	1.3725e-17
13	1.8840	0.7507	0.2461	72.4010	2.9376e-11	1.5532e-14	9.7129	2.1134e-20
14	1.6456	0.8476	0.0809	76.6722	1.6312e-07	6.8326e-13	9.6902	1.3079e-18
15	1.9994	0.6146	0.4998	108.5198	3.2942e-12	8.5399e-18	9.7245	1.6354e-16
16	1.9598	1.3700	0.0710	188.9893	1.2227e-07	7.5924e-08	9.6836	5.3382e-18
17	1.9999	0.5478	0.2567	63.1606	1.0011e-12	5.2160e-20	9.7193	1.3152e-17
18	2	1.3115	0.0673	148.3423	3.6112e-07	3.2618e-08	9.6843	1.4973e-16
19	1.4739	0.5323	0.1791	168.9302	1.5029e-07	6.5953e-21	9.6902	1.1615e-14
20	1.9225	0.7838	0.0588	66.3288	1.8026e-07	6.3978e-14	9.6885	4.9555e-17

Table 9. *Cont.*

Run	DOA				Analytical Method			Error (ϵ)
	m_1	m_2	R_s (Ω)	R_{sh} (Ω)	I_{s1} (A)	I_{s2} (A)	I_c (A)	
21	1.9432	0.5265	0.2173	65.8755	4.1640e-07	7.7455e-21	9.7119	6.1819e-17
22	2	0.5001	0.4326	81.9582	9.9875e-07	5.9915e-22	9.7311	9.3837e-18
23	1.9498	0.7612	0.0010	67.8896	8.6552e-07	2.3430e-14	9.6801	1.7277e-18
24	1.7804	1.1646	0.0484	93.4726	6.3280e-09	2.7793e-09	9.6850	3.3843e-18
25	2	0.5013	0.1490	62.3844	1.4445e-07	6.8580e-22	9.7031	3.2879e-17
26	2	1.2065	0.1408	161.4284	7.0345e-07	5.9391e-09	9.6884	1.8631e-18
27	1.9981	1.2430	0.1555	199.9746	2.2934e-07	1.1303e-08	9.6875	7.7431e-16
28	1.8329	1.2342	0.1258	199.9587	7.7650e-07	8.9471e-09	9.6860	4.1349e-19
29	1.4228	1.5533	0.0430	200	1.4494e-07	3.4957e-08	9.6820	5.2704e-15
30	1.8869	0.6304	0.4559	158.2097	8.6741e-07	2.2883e-17	9.7078	2.9661e-16

Table 10. DD model of thin-film Shell ST40 PV panel's optimal estimated parameters using DOA and analytical method.

Run	DOA				Analytical Method			Error (ϵ)
	m_1	m_2	R_s (Ω)	R_{sh} (Ω)	I_{s1} (A)	I_{s2} (A)	I_c (A)	
1	1.5337	0.5224	0.9630	60.6195	2.8984e-10	2.6833e-21	2.7225	2.9122e-19
2	1.9950	1.9695	0.2862	91.7166	1.5122e-08	6.7733e-06	2.6883	1.6850e-19
3	1.5738	0.9588	0.2969	64.9617	9.5282e-08	5.7604e-12	2.6922	1.4021e-19
4	1.7927	1.2757	0.8267	90.1395	8.5012e-07	3.6404e-09	2.7045	7.8745e-18
5	1.7581	1.6149	0.7695	96.0318	1.7189e-07	3.6506e-07	2.7014	5.4478e-17
6	1.7006	1.6202	0.6361	86.4797	1.7810e-07	3.4442e-07	2.6997	7.9361e-22
7	1.7268	1.9671	0.6621	139.2834	1.4930e-08	6.8429e-06	2.6927	1.5140e-17
8	1.8625	2	0.7590	189.6899	9.8681e-08	8.4479e-06	2.6907	3.0559e-17
9	1.9609	0.5022	0.2818	62.4350	3.8901e-07	3.5835e-22	2.6920	2.8063e-17
10	1.4998	1.3868	0.7457	77.8482	4.6590e-08	1.9246e-08	2.7056	1.4370e-18
11	1.9999	1.2008	0.2011	63.5729	1.2148e-07	1.7740e-09	2.6884	2.1936e-17
12	1.7096	0.5011	0.2120	61.2789	7.6222e-10	3.4104e-22	2.6892	7.9437e-19
13	1.9896	0.5933	0.4116	61.1869	3.1508e-08	8.4217e-19	2.6980	4.0059e-17
14	1.9815	1.1111	0.3436	64.3788	4.7572e-07	3.1011e-10	2.6943	9.2057e-18
15	1.8152	1.4450	0.0141	68.2482	8.4748e-07	3.8618e-08	2.6805	6.7612e-19
16	2	2	0.3566	99.7046	1.2391e-07	8.1947e-06	2.6895	1.1594e-16
17	1.8557	1.3175	0.0023	65.6913	6.1106e-07	9.1759e-09	2.6800	1.0629e-18
18	1.5496	1.9748	0.2055	87.3912	1.3397e-09	6.9365e-06	2.6863	5.0120e-19
19	1.6816	1.4256	0.9895	139.7725	7.2838e-07	4.2003e-09	2.6989	4.2693e-21
20	1.6349	1.2090	0.0032	63.6576	7.3524e-08	1.7453e-09	2.6801	1.3077e-19
21	2	0.5190	0.9018	62.8391	3.7291e-07	1.8721e-21	2.7184	3.6896e-16
22	2	0.9059	0.4616	63.2416	4.6508e-07	1.8429e-12	2.6995	1.0258e-17
23	1.7901	1.8366	0.1787	78.1192	5.0307e-07	1.9202e-06	2.6861	3.0518e-17
24	2	1.7622	0.9995	200	3.9830e-07	1.5223e-06	2.6934	3.9379e-18
25	1.7659	1.9976	0.8407	173.0700	8.0742e-07	4.3160e-06	2.6930	5.4780e-17
26	1.9742	1.9979	0.4966	114.8640	1.4283e-10	8.3194e-06	2.6915	7.8382e-16
27	1.9985	0.5398	0.0012	62.7582	6.9058e-07	1.1420e-20	2.6800	4.7297e-18
28	1.9985	2	0.6262	139.9758	8.1939e-07	7.7275e-06	2.6920	1.4919e-18
29	1.0491	1.9914	0.7876	199.9999	1.0000e-12	8.1763e-06	2.6905	1.2339e-16
30	1.8426	1.6893	0.9997	153.1942	1.8332e-09	8.4999e-07	2.6974	2.2748e-16

Monocrystalline SF430M

(**a**)

(**b**)

(**c**)

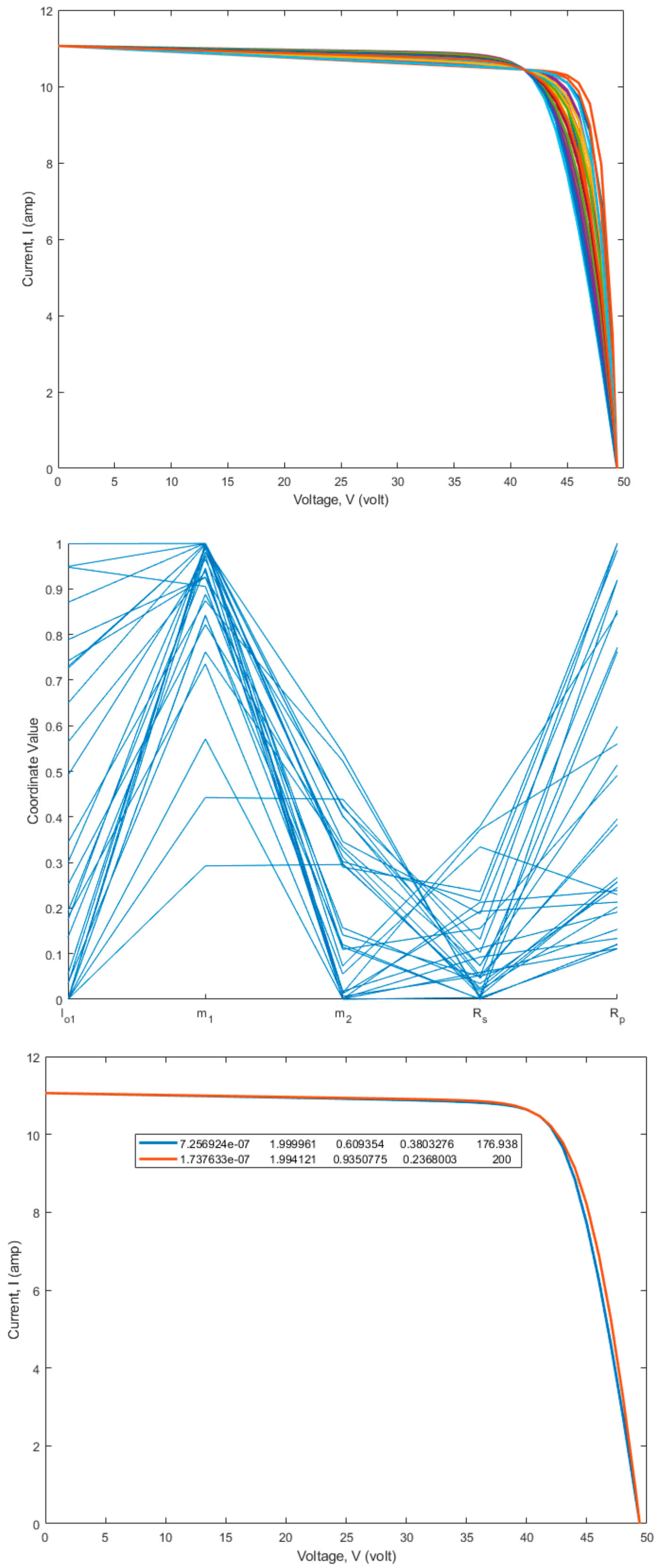

Figure 7. Simulation findings of parameter extraction of DD with monocrystalline SF430M PV panel: (**a**) *V*–*I* characteristics, (**b**) scatter plot, and (**c**) *V*–*I* characteristics with maximum R_s and R_{sh}.

Polycrystalline SG350P

(**a**)

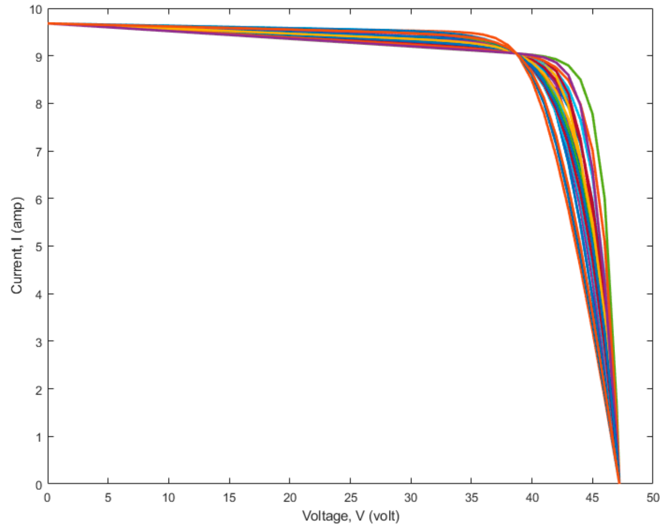

(**b**)

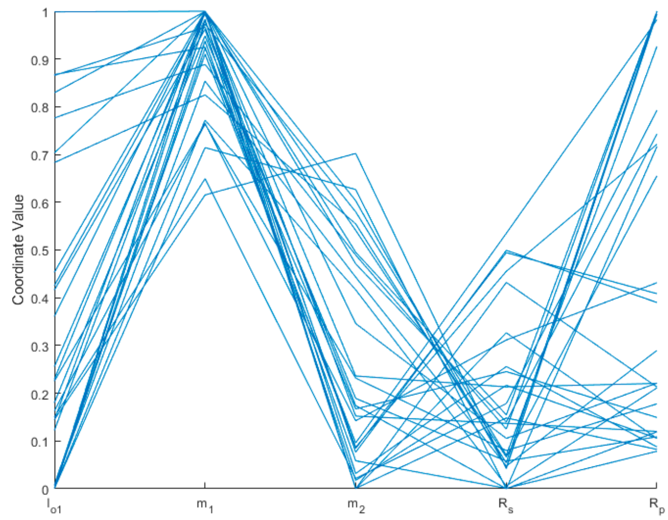

(**c**)

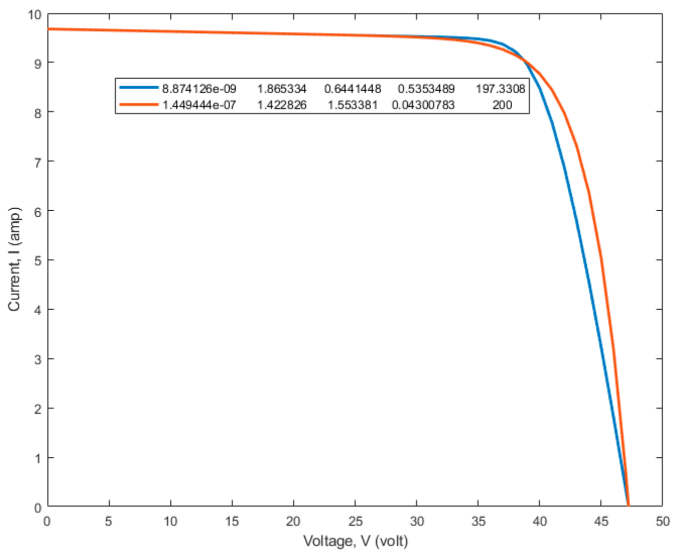

Figure 8. Simulation findings of parameter extraction of DD with polycrystalline SG350P PV panel: (**a**) *V–I* characteristics, (**b**) scatter plot, and (**c**) *V–I* characteristics with maximum R_s and R_{sh}.

Thin-film Shell ST40 PV

(**a**)

(**b**)

(**c**)

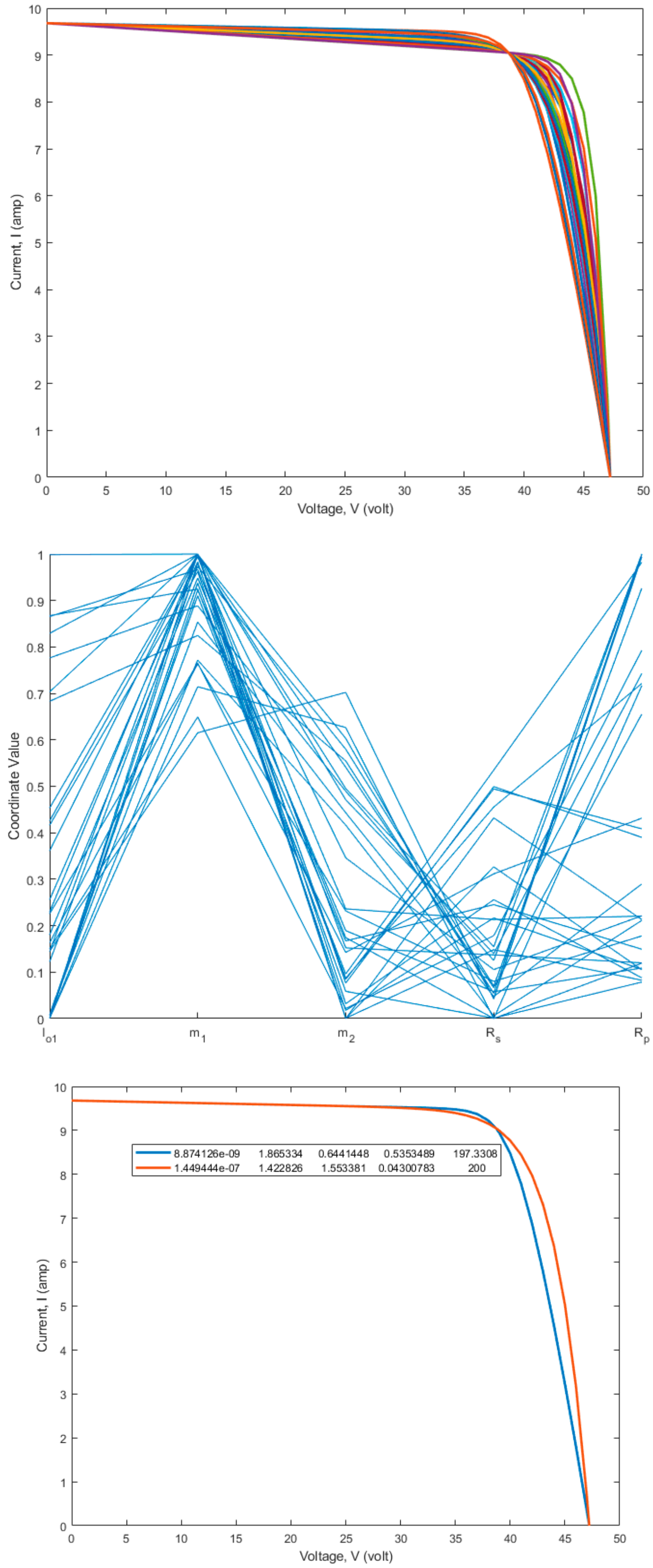

Figure 9. Simulation findings of parameter extraction of DD with thin-film Shell ST40PV panel: (**a**) *V*–*I* characteristics, (**b**) scatter plot, and (**c**) *V*–*I* characteristics with maximum R_s and R_{sh}.

From Figures 4a–9a of various PV panels, we can observe that all 30 V–I characteristics pass through three locations, which is the primary factor taken into account while designing the objective function. The error at three locations is almost negligible (10^{-16}), but in most of the investigations, the error is only considered at the MPP. As a result, all 30 runs produce essentially identical V–I characteristics with various conceivable parameter extractions. Figures 4b–9b of the various PV panels show the optimal solution set scatter plots. The optimal solutions, or V–I curves, obtained in each run are owed to various optimised parameters in the specified search space boundaries since the suggested algorithm is metaheuristic. Figures 4c–9c of the various PV panels show the V–I characteristics with the maximum R_s and R_{sh}. The slope of the curve at the OC and SC points is constrained by the values derived for the R_s and R_{sh}. It is clear from the data that the two curves that have the highest values of R_s and R_{sh} meet the main requirements by passing through all three crucial points of the features.

It is clear from the simulation results of the SD and DD models of various PV panels that the parameters estimated using the suggested DOA method ensure the accuracy of the V–I characteristics and that the three points acquired are in accordance with those in the datasheet.

Furthermore, Figure 10 displays the convergence curves of the SD and DD models of different PV panels, which are displayed using the optimal solution from 30 different studies conducted over 500 iterations. Clearly, the DOA achieved a quick convergence speed on each of the PV models.

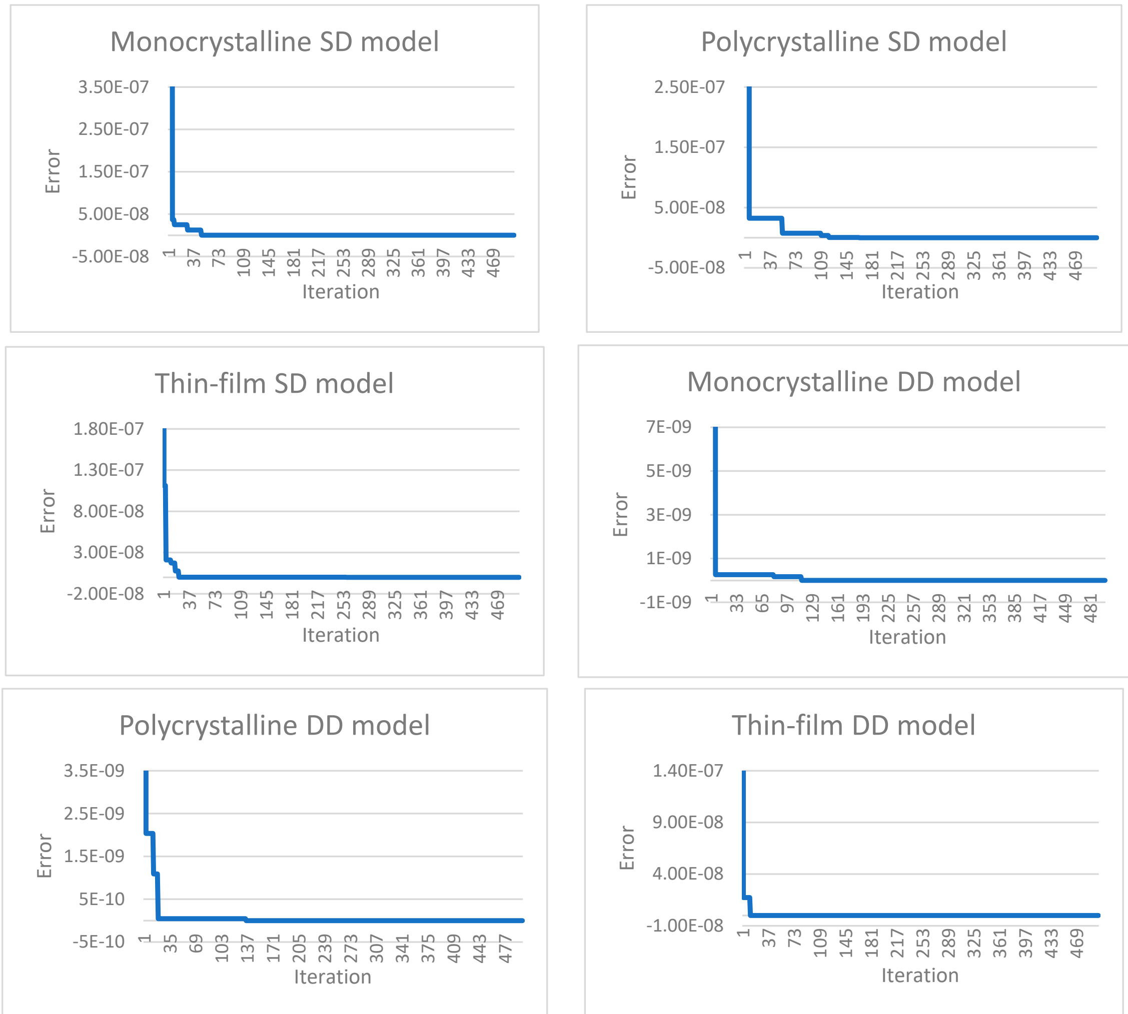

Figure 10. Convergence curves for SD and DD models of various PV panels.

In addition, a statistical evaluation of SD and DD models using the DOA in terms of standard deviation, sum, mean, and variance is presented in Table 11 and Figure 11 and compared with the HCSCA [5] and EHGWOSCA [6] algorithms. From Table 11 and Figure 11, we can observe that the standard deviation, sum, mean, and variance of the various PV panels using the DOA are lower compared to those of the other two hybrid algorithms. Therefore, we can conclude that the solar parameters obtained using the DOA are more accurate compared with the those obtained using the other two algorithms.

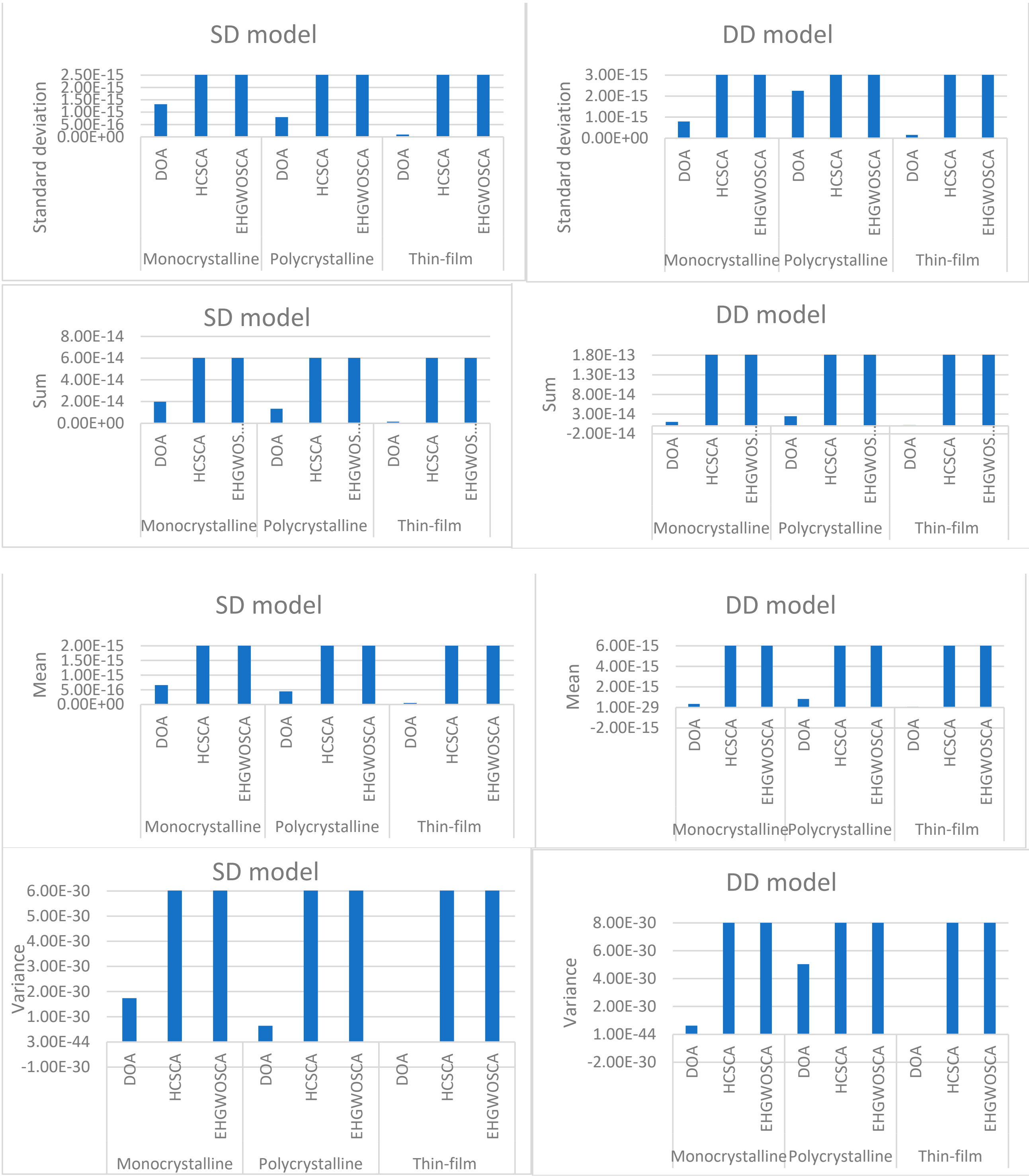

Figure 11. Statistical analysis curves for SD and DD models of various PV panels.

Table 11. Statistical evaluation of SD and DD models.

	Algorithm	DOA	HCSCA [5]	EHGWOSCA [6]	DOA	HCSCA [5]	EHGWOSCA [6]	DOA	HCSCA [5]	EHGWOSCA [6]
SD Model	Type of Solar PV		Monocrystalline			Polycrystalline			Thin Film	
	Commercial Solar PV	Mono SF430M	Mono CS6K280M	Mono CS6K280M	Poly SG350P	Poly KD210GH-2PU	Poly S75	Thin Film ST40	Thin Film ST40	Thin Film ST40
	Standard deviation	1.32e-15	2.38e-09	9.70e-12	8.00e-16	1.70e-09	4.55e-12	9.71e-17	3.53e-10	4.42e-13
	Count	30	30	30	30	30	30	30	30	30
	Sum	1.98e-14	5.22e-08	1.25e-10	1.34e-14	3.23e-08	5.03e-11	1.48e-15	6.50e-09	5.76e-12
	Mean	6.60e-16	1.74e-09	4.15e-12	4.46e-16	1.08e-09	1.68e-12	4.93e-17	2.17e-10	1.92e-13
	Variance	1.74e-30	5.65e-18	9.41e-23	6.41e-31	2.88e-18	2.07e-23	9.42e-33	1.25e-19	1.96e-25
DD Model	Algorithm	DOA	HCSCA [5]	EHGWOSCA [6]	DOA	HCSCA [5]	EHGWOSCA [6]	DOA	HCSCA [5]	EHGWOSCA [6]
	Type of Solar PV		Monocrystalline			Polycrystalline			Thin film	
	Commercial Solar PV	Mono SF430M	Mono CS6K280M	Mono CS6K280M	Poly SG350P	Poly KD210GH-2PU	Poly S75	Thin film ST40	Thin film ST40	Thin film ST40
	Standard deviation	7.91e-16	5.38e-08	5.06e-12	2.25e-15	0.0026917	2.07e-12	1.55e-16	6.18e-09	5.09e-13
	Count	30	30	30	30	30	30	30	30	30
	Sum	1.03e-14	7.26e-07	5.83e-11	2.48e-14	0.0153284	2.54e-11	1.94e-15	1.91e-07	5.34e-12
	Mean	3.45e-16	2.42e-08	1.94e-12	8.25e-16	0.0005109	8.47e-13	6.46e-17	6.37e-09	1.78e-13
	Variance	6.25e-31	2.89e-15	2.56e-23	5.04e-30	7.25e-06	4.27e-24	2.39e-32	3.81e-17	2.59e-25

7. Conclusions

A novel bio-inspired swarm-intelligence OA called the DOA has been proposed in this paper for extracting the parameters of SD and DD models of monocrystalline SF430M, polycrystalline SG350P, and thin-film Shell ST40 PV panels. In both SD and DD models, two parameters were calculated using an analytical approach, and the remaining parameters were obtained using the DOA. By reducing the objective function, the effectiveness of the suggested technique was assessed. The major findings of the proposed work are as follows:

1. The DOA yields more accurate results in over 30 trials with the specified error function as the objective function.
2. The simulation findings show that the parameters estimated provide *V*–*I* curves that pass through all three important points with approximately a 10e-22 error.
3. A statistical evaluation of SD and DD models using the DOA has been performed and they have been compared with two hybrid OAs. From the statistical analysis, we can observe that the standard deviation, sum, mean, and variance of various PV panels using the DOA are lower compared with those using the other two hybrid OAs.
4. The results show that the suggested algorithm produced adequate performance characteristics and that its practical ie was recommended.

Therefore, finally we conclude that the DOA has demonstrated to be a successful method of parameter estimation. By enhancing the suggested algorithm's performance with cutting-edge learning techniques, its application can also be expanded to the future parameter estimation of triple-diode PV panels.

Author Contributions: Conceptualisation, methodology, and software, T.C. and R.D.; formal analysis and investigation, R.I.V. and Ł.K.; writing—review and editing, T.C., K.S. and R.D.; funding acquisition, Ł.K. All authors have read and agreed to the published version of the manuscript.

Funding: This research was funded by the Polish Government, grant number 0212/SBAD/0594.

Institutional Review Board Statement: Not applicable.

Informed Consent Statement: Not applicable.

Data Availability Statement: Not applicable.

Conflicts of Interest: The authors declare no conflict of interest.

References

1. Esmaeili Shayan, M.; Najafi, G.; Ghobadian, B.; Gorjian, S.; Mazlan, M. Sustainable Design of a Near-Zero-Emissions Building Assisted by a Smart Hybrid Renewable Microgrid. *Int. J. Renew. Energy Dev.* **2022**, *11*, 471–480. [CrossRef]
2. Esmaeili Shayan, M.; Najafi, G.; Esmaeili Shayan, S. Microgrids Energy Management System Based on Renewable Energy. *Amirkabir J. Mech. Eng.* **2023**, *55*, 1–10.
3. Esmaeili Shayan, M.; Najafi, G.; Ghobadian, B.; Gorjian, S.; Mamat, R.; Fairusham Ghazali, M. Multi-microgrid optimization and energy management under boost voltage converter with Markov prediction chain and dynamic decision algorithm. *Renew. Energy* **2022**, *201*, 179–189. [CrossRef]
4. Esmaeili Shayan, M.; Najafi, G.; Ghobadian, B.; Gorjian, S.; Mazlan, M.; Samami, M.; Shabanzadeh, A. Flexible Photovoltaic System on Non-Conventional Surfaces: A Techno-Economic Analysis. *Sustainability* **2022**, *14*, 3566. [CrossRef]
5. Vandrasi, R.K.; Kumar, B.S.; Devarapalli, R. Solar photo voltaic module parameter extraction using a novel Hybrid Chimp-Sine Cosine Algorithm. *Energy Sources Part A Recovery Util. Environ. Eff.* **2022**, 1–20. [CrossRef]
6. Devarapalli, R.; Bathina, V.R.; Al-Durra, A. Optimal parameter assessment of Solar Photovoltaic module equivalent circuit using a novel enhanced hybrid GWO-SCA algorithm. *Energy Rep.* **2022**, *8*, 12282–12301. [CrossRef]
7. Jordehi, A.R. Parameter estimation of solar photovoltaic (PV) cells: A review. *Renew. Sustain. Energy Rev.* **2016**, *61*, 354–371. [CrossRef]
8. Bathina, V.R.; Devarapalli, R.; Malik, H.; Bali, S.K.; García Márquez, F.P.; Chiranjeevi, T. Wind integrated power system to reduce emission: An application of bat algorithm. *J. Intell. Fuzzy Syst.* **2022**, *42*, 1041–1049. [CrossRef]
9. Chiranjeevi, T.; Gupta, U.K. Ideal parameter distribution in renewable integrated rapid charging electric vehicle station. *Energy Sources Part A Recovery Util. Environ. Eff.* **2023**, *45*, 888–904. [CrossRef]
10. Knypiński, Ł.; Kuroczycki, S.; Marquez, F.P.G. Minimization of Torque Ripple in the Brushless DC Motor Using Constrained Cuckoo Search Algorithm. *Electronics* **2021**, *10*, 2299. [CrossRef]

11. Jervase, J.A.; Bourdoucen, H.; Al-Lawati, A. Solar cell parameter extraction using genetic algorithms. *Meas. Sci. Technol.* **2001**, *12*, 1922. [CrossRef]
12. Ye, M.; Wang, X.; Xu, Y. Parameter extraction of solar cells using particle swarm optimization. *J. Appl. Phys.* **2009**, *105*, 094502. [CrossRef]
13. Bisht, R.; Sikander, A. A novel way of parameter estimation of solar photovoltaic system. *COMPEL—Int. J. Comput. Math. Electr. Electron. Eng.* **2022**, *41*, 471–498. [CrossRef]
14. Naraharisetti, J.N.L.; Devarapalli, R.; Bathina, V. Parameter extraction of solar photovoltaic module by using a novel hybrid marine predators—Success history based adaptive differential evolution algorithm. *Energy Sources Part A Recovery Util. Environ. Eff.* **2020**, 1–23. [CrossRef]
15. Chen, X.; Yu, K. Hybridizing cuckoo search algorithm with biogeography-based optimization for estimating photovoltaic model parameters. *Sol. Energy* **2019**, *180*, 192–206. [CrossRef]
16. AlHajri, M.; El-Naggar, K.; AlRashidi, M.; Al-Othman, A. Optimal extraction of solar cell parameters using pattern search. *Renew. Energy* **2012**, *44*, 238–245. [CrossRef]
17. Sharma, A.; Dasgotra, A.; Tiwari, S.K.; Sharma, A.; Jately, V.; Azzopardi, B. Parameter Extraction of Photovoltaic Module Using Tunicate Swarm Algorithm. *Electronics* **2021**, *10*, 878. [CrossRef]
18. Biswas, P.P.; Suganthan, P.N.; Wu, G.; Amaratunga, G.A.J. Parameter estimation of solar cells using datasheet information with the application of an adaptive differential evolution algorithm. *Renew. Energy* **2019**, *132*, 425–438. [CrossRef]
19. Derick, M.; Rani, C.; Rajesh, M.; Farrag, M.; Wang, Y.; Busawon, K. An improved optimization technique for estimation of solar photovoltaic parameters. *Sol. Energy* **2017**, *157*, 116–124. [CrossRef]
20. Repalle, N.B.; Sarala, P.; Mihet-Popa, L.; Kotha, S.R.; Rajeswaran, N. Implementation of a Novel Tabu Search Optimization Algorithm to Extract Parasitic Parameters of Solar Panel. *Energies* **2022**, *15*, 4515. [CrossRef]
21. Singh, A.; Sharma, A.; Rajput, S.; Mondal, A.K.; Bose, A.; Ram, M. Parameter Extraction of Solar Module Using the Sooty Tern Optimization Algorithm. *Electronics* **2022**, *11*, 564. [CrossRef]
22. Guo, L.; Meng, Z.; Sun, Y.; Wang, L. Parameter identification and sensitivity analysis of solar cell models with cat swarm optimization algorithm. *Energy Convers. Manag.* **2016**, *108*, 520–528. [CrossRef]
23. Montoya, O.D.; Ramírez-Vanegas, C.A.; Grisales-Norena, L.F. Parametric estimation in photovoltaic modules using the crow search algorithm. *Int. J. Electr. Comput. Eng.* **2022**, *12*, 82–91. [CrossRef]
24. Saxena, A.; Sharma, A.; Shekhawat, S. Parameter extraction of solar cell using intelligent grey wolf optimizer. *Evol. Intell.* **2022**, *15*, 167–183. [CrossRef]
25. Louzazni, M.; Khouya, A.; Amechnoue, K.; Gandelli, A.; Mussetta, M.; Crăciunescu, A. Metaheuristic Algorithm for Photovoltaic Parameters: Comparative Study and Prediction with a Firefly Algorithm. *Appl. Sci.* **2018**, *8*, 339. [CrossRef]
26. Oliva, D.; Cuevas, E.; Pajares, G. Parameter identification of solar cells using artificial bee colony optimization. *Energy* **2014**, *72*, 93–102. [CrossRef]
27. Houssein, E.H.; Nageh, G.; Elaziz, M.A.; Younis, E. An efficient Equilibrium Optimizer for parameters identification of photovoltaic modules. *PeerJ Comput. Sci.* **2021**, *7*, e708. [CrossRef] [PubMed]
28. Kashefi, H.; Sadegheih, A.; Mostafaeipour, A.; Mohammadpour Omran, M. Parameter identification of solar cells and fuel cell using improved social spider algorithm. *COMPEL—Int. J. Comput. Math. Electr. Electron. Eng.* **2021**, *40*, 142–172. [CrossRef]
29. Abdel-Basset, M.; Mohamed, R.; El-Fergany, A.; Askar, S.S.; Abouhawwash, M. Efficient Ranking-Based Whale Optimizer for Parameter Extraction of Three-Diode Photovoltaic Model: Analysis and Validations. *Energies* **2021**, *14*, 3729. [CrossRef]
30. Shaheen, A.; El-Sehiemy, R.; El-Fergany, A.; Ginidi, A. Representations of solar photovoltaic triple-diode models using artificial hummingbird optimizer. *Energy Sources Part A Recovery Util. Environ. Eff.* **2022**, *44*, 8787–8810. [CrossRef]
31. Al-Shamma'a, A.A.; Omotoso, H.O.; Alturki, F.A.; Farh, H.M.H.; Alkuhayli, A.; Alsharabi, K.; Noman, A.M. Parameter Estimation of Photovoltaic Cell/Modules Using Bonobo Optimizer. *Energies* **2022**, *15*, 140. [CrossRef]
32. Gao, X.; Cui, Y.; Hu, J.; Xu, G.; Yu, Y. Lambert W-function based exact representation for double diode model of solar cells: Comparison on fitness and parameter extraction. *Energy Convers. Manag.* **2016**, *127*, 443–460. [CrossRef]
33. Chegaar, M.; Ouennoughi, Z.; Hoffmann, A. A new method for evaluating illuminated solar cell parameters. *Solid-State Electron.* **2001**, *45*, 293–296. [CrossRef]
34. Reddy, S.S.; Yammani, C. Parameter extraction of single-diode photovoltaic module using experimental current–voltage data. *Int. J. Circuit Theory Appl.* **2021**, *50*, 753–771. [CrossRef]
35. Louzazni, M.; Aroudam, E.H. An analytical mathematical modeling to extract the parameters of solar cell from implicit equation to explicit form. *Appl. Sol. Energy* **2015**, *51*, 165–171. [CrossRef]
36. Muhammadsharif, F.F. A New Simplified Method for Efficient Extraction of Solar Cells and Modules Parameters from Datasheet Information. *Silicon* **2022**, *14*, 3059–3067. [CrossRef]
37. Gong, C.; Han, S.; Li, X.; Zhao, L.; Liu, X. A new dandelion algorithm and optimization for extreme learning machine. *J. Exp. Theor. Artif. Intell.* **2018**, *30*, 39–52. [CrossRef]
38. Li, X.; Han, S.; Zhao, L.; Gong, C.; Liu, X. New dandelion algorithm optimizes extreme learning machine for biomedical classification problems. *Comput. Intell. Neurosci.* **2017**, *2017*, 4523754. [CrossRef] [PubMed]
39. Zhao, S.; Zhang, T.; Ma, S.; Chen, M. Dandelion Optimizer: A nature-inspired metaheuristic algorithm for engineering applications. *Eng. Appl. Artif. Intell.* **2022**, *114*, 105075. [CrossRef]

40. SF430M Peimar Monocrystalline Solar Panels Datasheet. Available online: https://www.enfsolar.com/pv/panel-datasheet/crystalline/51664 (accessed on 1 July 2022).
41. SG350P Peimar Polycrystalline Solar Panels Datasheet. Available online: https://www.enfsolar.com/pv/panel-datasheet/crystalline/51661 (accessed on 1 July 2022).
42. Soon, J.J.; Low, K.S. Photovoltaic Model Identification Using Particle Swarm Optimization with Inverse Barrier Constraint. *IEEE Trans. Power Electron.* **2012**, *27*, 3975–3983. [CrossRef]